OPEN ACCESS

ORIGINAL RESEARCH

Efficient acute and chronic infection of stem cell-derived hepatocytes by hepatitis C virus

Arnaud Carpentier ,[1,2] Julie Sheldon,[1] Florian W R Vondran,[3,4] Richard JP Brown,[1,5] Thomas Pietschmann[1,2,4]

► Additional material is published online only. To view, please visit the journal online (http://dx.doi.org/10.1136/gutjnl-2019-319354).

[1]Institute of Experimental Virology, Twincore, Hannover, Germany
[2]Cluster of Excellence RESIST (EXC 2155), Hannover Medical School, Hannover, Germany
[3]ReMediES, Department of General, Visceral and Transplant Surgery, Hannover Medical School, Hannover, Germany
[4]German Centre for Infection Research (DZIF), partner site Hannover-Braunschweig, Germany
[5]Division of Veterinary Medicine, Paul-Ehrlich-Institut, Langen, Germany

Correspondence to
Dr Arnaud Carpentier, Twincore, Hannover, Germany; arnaud.carpentier@twincore.de
Professor Thomas Pietschmann; thomas.pietschmann@twincore.de

Received 26 June 2019
Revised 7 February 2020
Accepted 10 February 2020
Published Online First 29 February 2020

► http://dx.doi.org/10.1136/gutjnl-2020-321216

To cite: Carpentier A, Sheldon J, Vondran FWR, *et al*. *Gut* 2020;**69**:1659–1666.

ABSTRACT

Objective and design Human stem cell-derived hepatocyte-like cells (HLCs) have shown high potential as authentic model for dissection of the HCV life cycle and virus-induced pathogenesis. However, modest HCV replication, possibly due to robust innate immune responses, limits their broader use. To overcome these limitations and to dissect the mechanisms responsible for control of HCV, we analysed expression of key components of the interferon (IFN) system in HLCs, assessed permissiveness for different HCV strains and blocked innate immune signalling by pharmacological intervention.

Results Transcriptional profiling revealed that HLCs constitutively express messenger RNA of RLRs, and members of the IFN pathway. Moreover, HLCs upregulated IFNs and canonical interferon-regulated genes (IRGs) upon transfection with the double-stranded RNA mimic poly(I:C). Infection of HLCs with Jc1-HCVcc produced only limited viral progeny. In contrast, infection with p100, a Jc1-derived virus population with enhanced replication fitness and partial resistance to IFN, resulted in robust yet transient viraemia. Viral titres declined concomitant with a peak of IRG induction. Addition of ruxolitinib, a JAK/STAT inhibitor, permitted chronic infection and raised p100 infectious virus titres to 1×10^5 FFU/mL. IRGs expression profiling in infected HLCs revealed a landscape of HCV-dependent transcriptional changes similar to HCV-infected primary human hepatocytes, but distinct from Huh-7.5 cells. Withdrawal of ruxolitinib restored innate immune responses and resulted in HCV clearance.

Conclusion This authentic human cell model is well suited to examine acute and chronic host-HCV interactions, particularly IFN-triggered antiviral effector functions and mechanisms of innate immune control of HCV infection.

Significance of this study

What is already known on this subject?
- Stem cell-derived hepatocyte-like cells (HLCs) represent a relatively mature model of hepatocytes.
- HLCs are permissive to HCV infection, but infection efficiency is low.
- Primary human hepatocytes are susceptible to HCV infection, however, rapid de-differentiation and donor-to-donor variation complicate analyses.

What are the new findings?
- Inoculation of HLCs with cell culture-adapted p100 HCV population allows complete and efficient replication of the virus.
- HLCs clear acute HCV infection by a robust innate immune response, which is comparable to the one observed in primary adult hepatocytes.
- Blockade of JAK/STAT signalling permits chronic HCV infection of HLCs, time-dependent experimental control of the innate immune response and thus analysis of effector functions mediating viral clearance.

How might it impact on clinical practice in the foreseeable future?
- Our findings establish stem cell-derived HLCs and p100 infection as tractable and authentic model for studying of acute and chronic host-HCV interactions.
- They open the way to personalised cell culture models of HCV infection, potentially providing critical insights for future personalised infection medicine.

INTRODUCTION

Although efficient direct-acting antivirals (DAAs) are available, HCV infection remains a global health problem, with ca. 70 million chronically infected patients.[1 2] HCV vaccine development represents an important research goal, and benefits from a comprehensive understanding of the characteristics of protective immunity to HCV as well as the mechanisms of viral innate and adaptive immune evasion. These aspects have been heavily investigated using in vitro models for propagation of HCV relying mainly on the use of the Huh-7.5 hepatoma cell line. Notably, Huh-7.5 cells encode a defective retinoic acid inducible gene I (RIG-I), and therefore exhibit a blunted innate immunity,[3] making them unsuitable for investigation of innate immune mechanisms associated with HCV clearance or persistence. Cultures of primary human hepatocytes (PHHs) are generally permissive to HCV in vitro infection[4] and represent a more mature model to analyse innate immunity in response to HCV infection.[5 6] However, PHHs present important limitations: limited availability, donor-specific differences in permissiveness, short duration of culture and de-differentiation on in vitro culture.

Human pluripotent stem cells (embryonic (hESCs) or induced (hiPSCs)) can be differentiated in vitro into cells reproducing key features of hepatocytes.[7] These cells, termed hepatocyte-like cells (HLCs), are permissive to HBV,[8 9] HCV[10–13] and HEV[14] infection in vitro. Upon inoculation with cell culture-derived HCV (HCVcc) containing the JFH1 (Gt2a) replication machinery,[15] HLCs yield detectable intracellular HCV RNA replication, but only limited and transient production of infectious progeny viruses. It is generally assumed that active innate immunity is responsible for this acute HCV infection.[16–18]

The HCV genome replicates via the formation of a viral double-stranded (ds)RNA, a hallmark of viral replication, sensed by cellular pattern recognition receptors (PRRs). Among them are toll-like receptors (TLRs), particularly TLR3 detecting endosomal dsRNA,[19] and the RIG-I-like receptors (RLRs) RIG-I[20 21] and MDA5[20 22 23] detecting cytoplasmic dsRNA and signalling through the adaptor protein MAVS. Upon triggering, these PRRs induce interferon regulatory factor (IRF)3 translocation and interferon (IFN) production. Upon binding of type I or type III IFN to the cell surface receptors, the JAK/STAT signalling cascade activate transcription of numerous interferon-regulated genes (IRGs) controlling HCV infection.[24 25] Among previously described IRGs with anti-HCV action are the PRRs MDA5 and RIG-I,[26] ISG 15[27] and MXA.[28] Modulation of the JAK/STAT signalling pathway in HLCs has been previously described in order to improve HEV[14] and HCV[16–18] infection, but with conflicting results reported.[17] Another approach to improve viral replication is to use HCVcc virus populations, selected for higher viral replication in Huh7-derived cell lines. Among them, a recently characterised Jc1-derived HCVcc viral population (termed p100) was isolated by long-term passage in Huh-7.5 cells; p100 exhibits higher replicative capabilities and partial resistance to IFN.[29 30]

Here, we infected HLCs with parental and adapted HCVcc and monitored innate immune responses during acute infection. We compared their innate immune response with the one in PHHs and Huh-7.5 cells, and investigated pharmacological intervention to modulate it, in order to make this model more tractable and valuable to decipher IFN-based antiviral effector functions and cellular mechanisms involved in viral clearance or persistence.

MATERIALS AND METHODS

See online supplementary materials.

RESULTS

HLCs possess an inducible, hepatocyte-like, innate immunity

HLCs were produced using standard protocols (online supplementary figures S1 and S2).[12 31] They expressed key viral PRRs, IFN receptors and genes involved in the IFN pathway (online supplementary figure S3). HLCs can sense dsRNA through their RLRs, leading to IRF3 translocation, production of IFNs and subsequent induction of IRGs, making them a potential valuable model to analyse the innate immune response to HCV (online supplementary figure S4).

HCVcc p100 infection of HLCs and IRGs induction

HLCs were infected with the cell culture adapted p100 HCV virus population (figure 1A), resulting in enhanced viral replication when compared with the Jc1 parent virus (online supplementary figure S5). DAAs completely abrogated production of progeny p100 virus (online supplementary figures S5 and S6). Interestingly, treatment with ruxolitinib, a JAK/STAT pathway inhibitor (JSi), led to higher p100 viral replication, in HLCs (online supplementary figures S5 and S6) and PHHs (online supplementary figure S8) suggesting an important role of cellular innate immunity during acute p100 HCV infection of HLCs and PHHs.

Infectious titres and production of IFNs and selected IRGs were concomitantly monitored during acute infection of HLCs by p100 HCV, in the presence or absence of ruxolitinib. During the initial days post infection (pi), infectious titres increased gradually to reach 10^4 FFU/mL in both ruxolitinib-treated and ruxolitinib-untreated infected HLCs (figure 1). However, in the following days, the titres decreased and infectivity was sometimes not detectable anymore at d11pi in non-treated cells, while in ruxolitinib-treated HLCs, infectious virions production did not decline, and titres reached up to 10^5 FFU/mL at d11pi. In infected HLCs, IRG messenger RNA (mRNA) induction (figures 1 and 2) and protein expression (figure 1C–D and online supplementary figure S6C) remained low during the first 4 days pi, followed by a rapid burst of induction, correlating with >100-fold drop of infectious virus titres. IRF3 nuclear translocation could sometimes be observed in HCV NS5A-positive HLCs (figure 1E), and type I and III IFNs upregulation was detectable concomitant with upregulation of IRGs and HCV clearance (figure 1F). Notably, very little, if any induction of IFN mRNAs was observed when infected HLCs were treated with ruxolitinib, suggesting that JAK/STAT-dependent feedback is necessary for full induction of type I and III IFN mRNA in this system. Importantly, ruxolitinib treatment did not affect levels of hepatic maturation or the expression of HCV-associated host factors in HLCs (online supplementary figure S7). Similar data were obtained when PHHs were infected with HCV p100 and treated with ruxolitinib (online supplementary figure S8).

Transfection of HLCs with siRNA against STAT1, but not STAT2 (figure 2A), and blocking of the IFN receptor complex using anti-IFN-alpha receptor (IFNAR) antibodies (figure 2B) increased production of infectious progeny viruses, confirming that inhibition of the IFNAR signalling enhances HCV p100 infection of HLCs.

We previously reported that p100 HCV infection causes enhanced PKR activation compared with Jc1 infection.[29] Moreover, other groups postulated that activation of PKR may be proviral by inhibiting translation of IFNs and IRGs.[32–34] Therefore, we investigated the influence of PKR activation on p100 infection of HLCs by using oxindole-imidazole C16, a PKR inhibitor.[35] C16 treatment decreased p100 replication on day 4 post inoculation, suggesting a proviral effect of PKR (figure 2C–D). However, at later time points, concomitant with massive induction of IRGs (figure 2E), C16 no longer inhibited infection. These results suggest a time-dependent role of PKR activation for control of p100 HCV infection of HLCs.

RNA-Seq analysis of HLCs infected with p100

To globally assess HCV-mediated innate immune activation, we performed RNA-Seq analyses of infected HLCs, with or without ruxolitinib or telaprevir, and compared them with uninfected HLCs. Expression levels of cellular mRNAs were quantified by mapping reads to the hg19 reference genome and normalisation performed to allow comparison between experiments. Normalised expression values for individual genes are presented as the number of Reads Per Kilobase of transcript, per Million mapped reads (RPKM). Analyses were performed at time points when infectious titre in infected, non-JSI-treated cells were dropping (online supplementary table S1, GEO accession GSE132606).

Pathway analyses showed that IFN response and other innate immune pathways are the most prominently dysregulated pathways on HCV infection of HLCs (figure 3A) (online

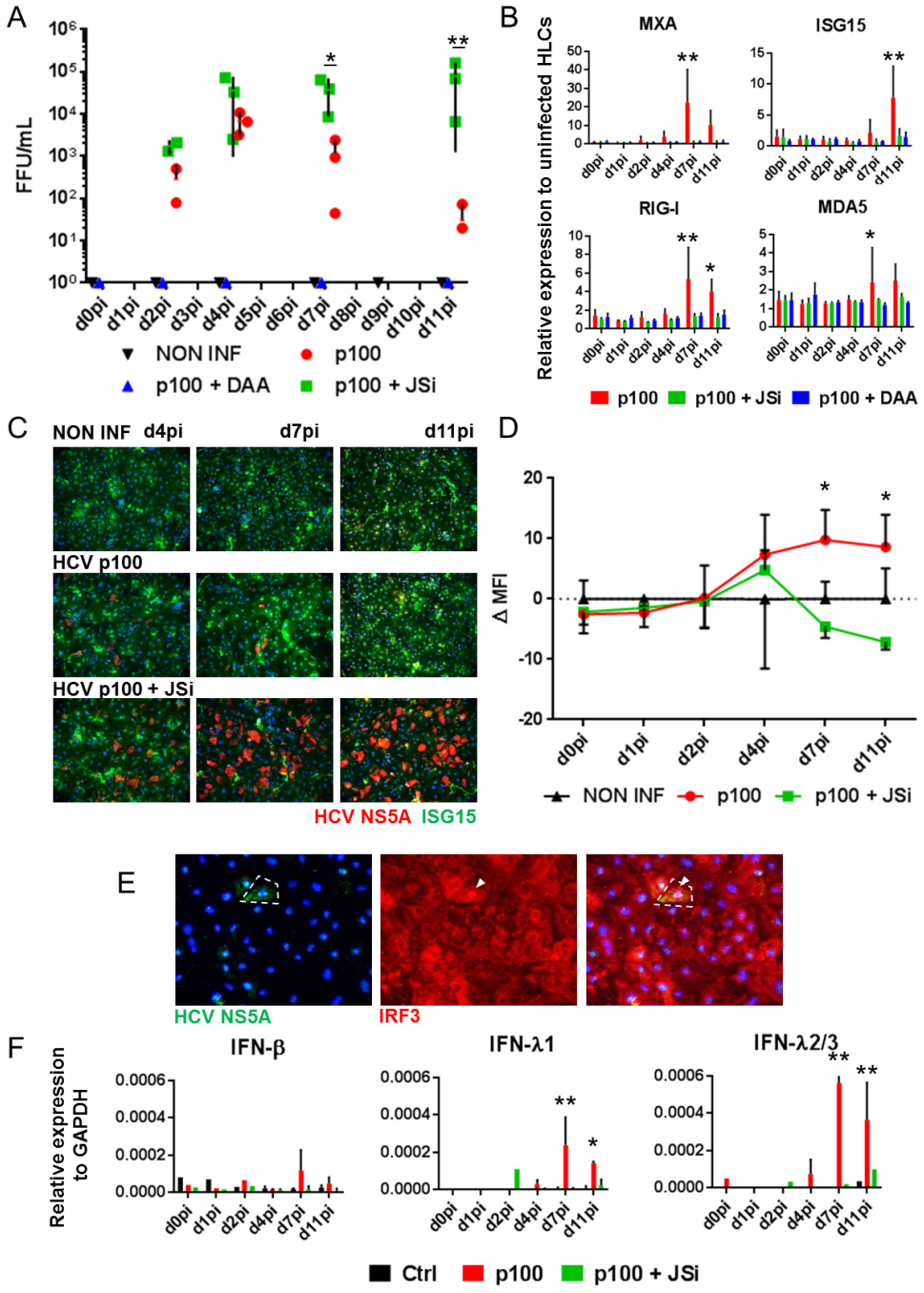

Figure 1 Time and JAK/STAT-dependent control of stem cell-derived hepatocyte-like cell (HLC) infection by HCV p100. HLCs were left untreated (black) or inoculated with p100 (Multiplicity of Infection (MOI): 1) in presence of solvent (red), Telaprevir (direct-acting antiviral (DAA), blue) or ruxolitinib (JAK/STAT pathway inhibitor (JSi), green). (A) Kinetics of infectious virus production in supernatants of infected HLCs. (B) Time-dependent and treatment-dependent induction of selected interferon-regulated genes (IRGs), monitored by RT-qPCR, and expressed relative to uninfected cells. (C) Immunostaining for ISG15 and HCV NS5A in p100-inoculated HLCs. (D) Mean fluorescent intensity quantification of ISG15 staining in panel C. (E) HCV NS5A and interferon regulatory factor (IRF)3 co-staining on p100-infected HLCs, 7 dpi. (F) Type I and III interferon (IFN) induction on HCV p100 infection of HLCs. Means with SD of 3 independent experiments are given, statistical significance: *p<0.05; **p<0.01.

supplementary figure 9A-C)(online supplementary tables S2 and S3). Upon ruxolitinib or DAA treatment, no immune-related pathways were enriched, indicating the dominance of HCV-triggered innate immune response pathways and highlighting replication-dependent triggering of these pathways.

Our dataset was then analysed for 417 IRGs, including 112 IRGs associated with HCV and other flaviviruses infection.[24–26] The total list of analysed IRGs and their differential expression on HCV infection can be found in online supplementary figure S10A and online supplementary table S4. In the infected HLCs, 46 of the 417 analysed IRGs were upregulated more than two fold (figure 3B, 'HCV'), when compared with control cells (figure 3B, 'NINF'). Among them are the IRF7 and IRF9, and IRGs previously described as restricting HCV infection (IFI27, IFI44L, IFITM1, IFITM3, ISG15, MXA, the oligoadenylate synthetase system components OAS1, OAS2 and OAS3, OASL, RSAD2 (viperin) and BST2 (tetherin)). IRG upregulation was strongly inhibited in infected cells treated with telaprevir

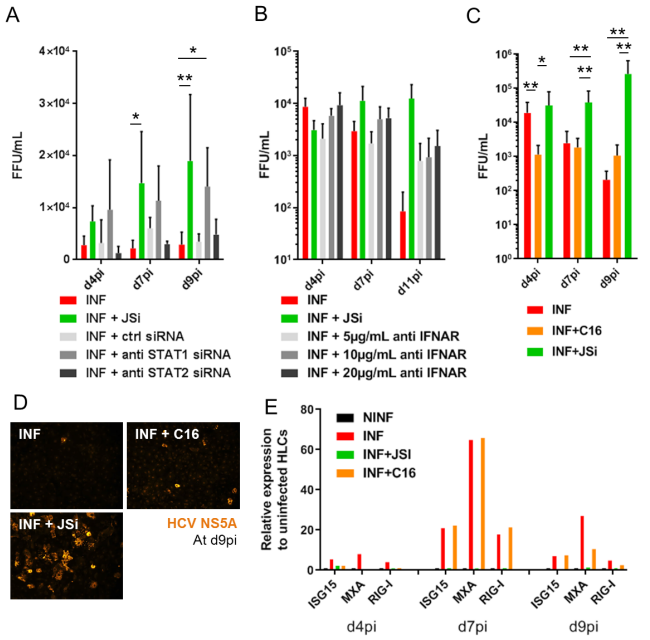

Figure 2 Modulation of p100 HCV replication in stem cell-derived hepatocyte-like cells (HLCs). Production of infectious progeny in p100 HCV-infected HLCs (A) transfected with small interfering RNA (siRNA) against STAT1 and STAT2, (B) pre-incubated with anti-IFN-alpha receptor (anti IFNAR) antibodies, (C) treated with the PKR inhibitor C16, compared to non treated or Ruxolitinib (JSi)-treated HLCs. (D) Visualisation of infected HLCs, treated or not with C16 and/or JSi, 9 days post inoculation. (E) Interferon-regulated genes (IRGs) induction in HLCs treated or not with C16 or JSi. Means with SD of 2 (A, B) or 4 (C) independent experiments are given, statistical significance: *p<0.05; **p<0.01.

(figure 3B, 'DAA') or ruxolitinib (figure 3B, 'JSi'), confirming that on sensing of the replicating viral RNA, the JAK/STAT and IFN pathways are critical for induction of IRGs and their subsequent antiviral effect.

A rank ordered mRNA expression analysis confirms that upon HCV infection, HLCs upregulate many IRGs (figure 3C), particularly IRGs with described anti-HCV properties expressed only at very low level (RPKM <0.05) in control cells (figure 3C, red dots). HCV infection induced expression of some IRGs, which are not, or only partially dependent on JAK/STAT signalling, as ruxolitinib treatment of p100-inoculated HLCs did not totally ablate their induction. This group of mRNAs includes OASL, RTP4 and IFIT2 (online supplementary figure S10 and figure 3C, green dots). Moreover, induction of the RLRs RIG-I and MDA5 depended on JAK/STAT signalling offering a possible explanation why ruxolitinib treatment affected HCV-dependent induction of type I and III IFN mRNAs (figure 1F) (online supplementary table S4B, C).

HLCs innate immunity is comparable to the one of PHHs

We then compared expression and induction of IRGs in our HLCs with the one in Huh-7.5 cells and in PHHs (online supplementary figure S9D–F), using comprehensive RNA-Seq datasets reported elsewhere (Tegtmeyer B and Vieyres G *et al*, manuscript in revision; GEO accession: GSE132548). As described above, upon HCV infection, HLCs upregulate 46 IRGs, while PHHs and Huh-7.5 cells upregulate 159 and 53 IRGs, respectively (figure 4A) (online supplementary table S4 and S5). Forty-three of the 46 IRGs upregulated in HLCs were also upregulated in PHHs (figure 4A–C) while IRGs upregulated in infected Huh-7.5 cells were mostly distinct from the one upregulated in HLCs and PHHs (figure 4B,C). Ten IRGs were upregulated in all three models, among them were the PRR MDA5 (IFIH1), MX1 and ISG15. The pattern and intensity of IRGs upregulation upon HCV infection in HLCs correlated better with the one observed in PHHs (r=0.3124) than with the one in Huh-7.5 cells (r=0.0562) (figure 4D). Huh-7.5 IRG upregulation was also poorly correlated with the response in PHHs (r=0.0133). Importantly, both basal and induced levels of expression of IRGs in Huh-7.5 cells were very low compared with PHHs and HLCs (figure 4E). Taken together, these results confirm that Huh-7.5 cells represent a poor model to analyse innate immune response to HCV. HLCs on the other hand are a good substitute model to the innate immune activation of the native host cell of HCV, the PHH.

Experimentally controlled clearance of chronic HLC infection by HCV p100

We then examined if it is possible to establish a chronic, long-term HCV infection of HLCs. We previously described that HLCs could be maintained for several weeks[31] and could support chronic infection with HBV.[9] In the present study, we maintained HLCs for 3 weeks, with only limited loss of hepatic maturation (online supplementary figure S11). The HLCs maintained an active lipoprotein secretion pathway (online supplementary figure S11D), an important host factor for production of infectious progeny viruses. Ruxolitinib had no effect on the level of maturation of the cells even after 3 weeks of treatment (online supplementary figure S11A,C).

When HLCs were infected with p100 HCV and cultured without ruxolitinib, the induction of innate immune responses cleared the virus within 2 weeks (figure 5A,B, red). On the other hand, when kept under ruxolitinib treatment, p100 infection was maintained with constant infectious virus production for at least 21 days (figure 5A, dark green), without IRG induction (figure 5B). If ruxolitinib was removed from the culture medium (figure 5A,C, arrowhead), infectious titres subsequently dropped (figure 5A, light green line), concomitant with an induction of IRGs (figure 5C) mimicking the innate immune response observed at earlier time points in infected non-treated HLCs (figure 5B).

Taken together, these data show that the innate immune response to HCV infection can be controlled by using ruxolitinib, thus permitting a chronic HCV infection. Withdrawal of ruxolitinib experimentally restores innate immunity and control of the infection, making this a valuable tool to monitor and manipulate the hepatocyte innate immune response to HCV.

DISCUSSION

Here, we report that stem cell-derived HLCs represent a tractable and immunocompetent model for the study of the cellular response to HCV. Tailored use of ruxolitinib, an inhibitor of the JAK/STAT signalling pathway, allows experimentally controlled induction of innate immunity and in turn viral clearance or persistence.

HCV infection studies in HLCs are challenging due to low infection rates and poor replication levels. In this regard, utilisation of p100, a Jc1-derived virus population with elevated fitness in Huh-7.5 cells is a key improvement, as infection with this virus population permits robust recapitulation of the entire viral life cycle in HLCs. It is not clear which features of p100 are important for mediating enhanced infection rate in the HLC culture. Sequencing analysis of p100 revealed nine coding mutations across the viral polyprotein.[29] Four of them map to

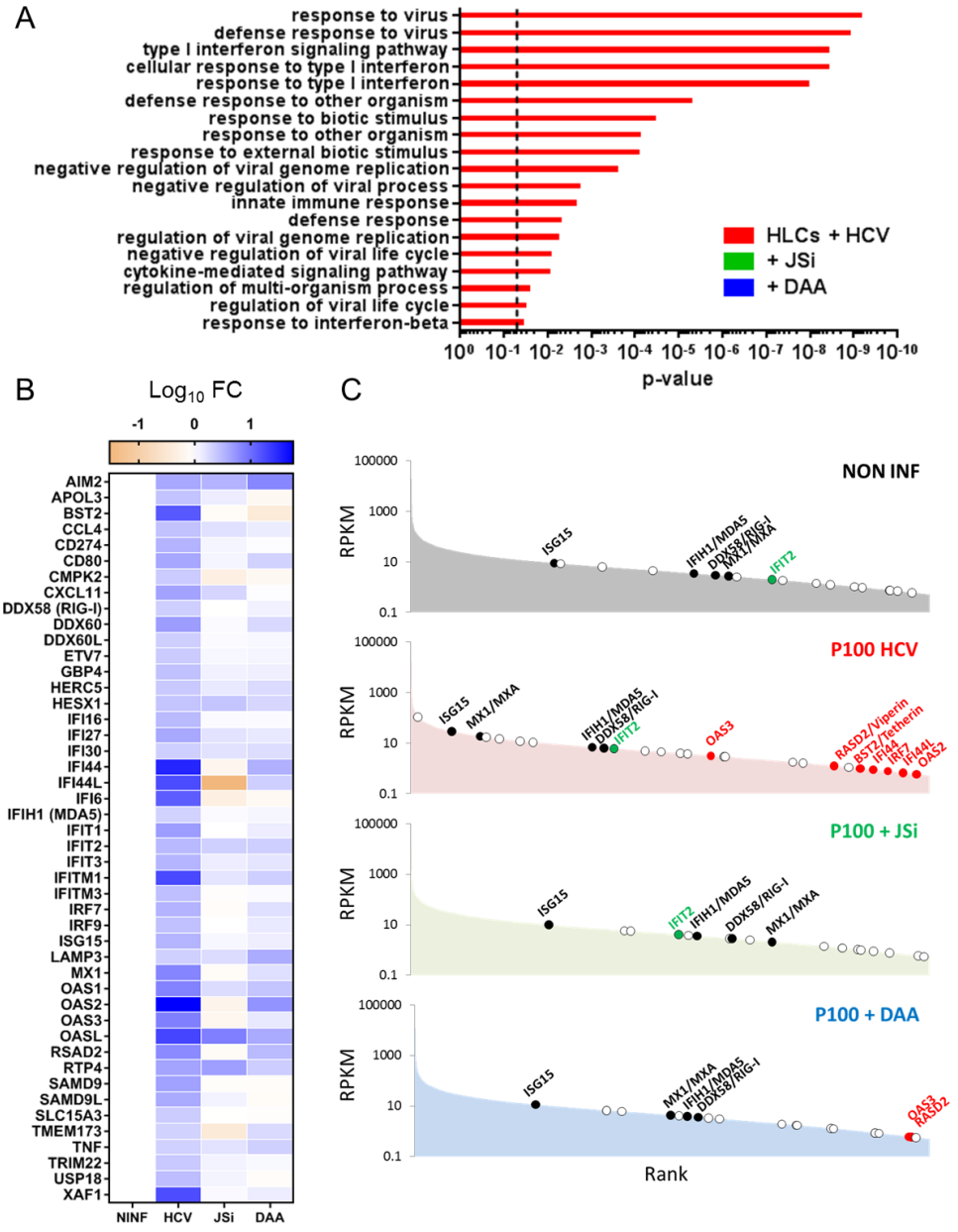

Figure 3 RNA-Seq analyses of p100-infected stem cell-derived hepatocyte-like cells (HLCs) (HCV), treated or not with 10 µM telaprevir (direct-acting antiviral (DAA)) or ruxolitinib (JAK/STATpathway inhibitor (JSi)), compared with non-infected HLCs. (A) Most upregulated pathways according to the Gene Ontology (GO) Enrichment Analysis tool. Histograms show p value calculated with Bonferroni correction. Dotted line indicates p value of 0.05. (B) Induction of selected interferon-regulated genes (IRGs) in each condition, expressed as $\log_{10}$ fold change of 'Reads Per Kilobase of transcript, per Million mapped reads' (RPKM) values compared with uninfected HLCs. Total list of studied IRGs can be found in online supplementary figure S10A. (C) RPKM ranking of selected IRGs in non-infected HLCs, p100-infected HLCs and infected HLCs treated with JJSi or telaprevir (DAA).

the NS3-4A protease complex, the NS5A phosphoprotein and the NS5B RNA-dependent RNA polymerase, and may directly affect RNA replication, and/or presentation of viral dsRNA to cellular PRRs. The point mutation in NS5A, a protein that has been implicated in inhibiting PKR function,[36] could modify PKR-dependent repression of innate immunity.[32–34] In line with this notion, p100 infection of Huh-7.5 cells is associated with enhanced phosphorylation of PKR and cellular protein translation shut off.[29] Treatment of HLCs with the C16 PKR inhibitor decreased replication of p100 during the first days pi, suggesting that PKR activation may participate in the initial establishment of the p100 infection of HLCs. However, at later time points, C16 no longer exerted a significant effect. Collectively, these findings imply that viral determinants govern infection efficiency in this model and that early activation of PKR may facilitate infection. A broader comparison of HCV strains including primary virus populations from patients could help to characterise viral features critical for infection of these cells.

Modulation of the JAK/STAT pathway has been discussed previously as a way to improve viral replication in HLCs.[16–18] Here, we monitored in detail the induction of innate immunity and its influence, on the complete replication cycle over extended periods. To modulate the JAK/STAT pathway, we used ruxolitinib, a kinase inhibitor that may have additional effects on the treated cells. However, analyses of gene expression data excluded a major impact of ruxolitinib on the level of HLC maturation, or expression of HCV replication co-factors (online supplementary figure S7). We also showed that ruxolitinib

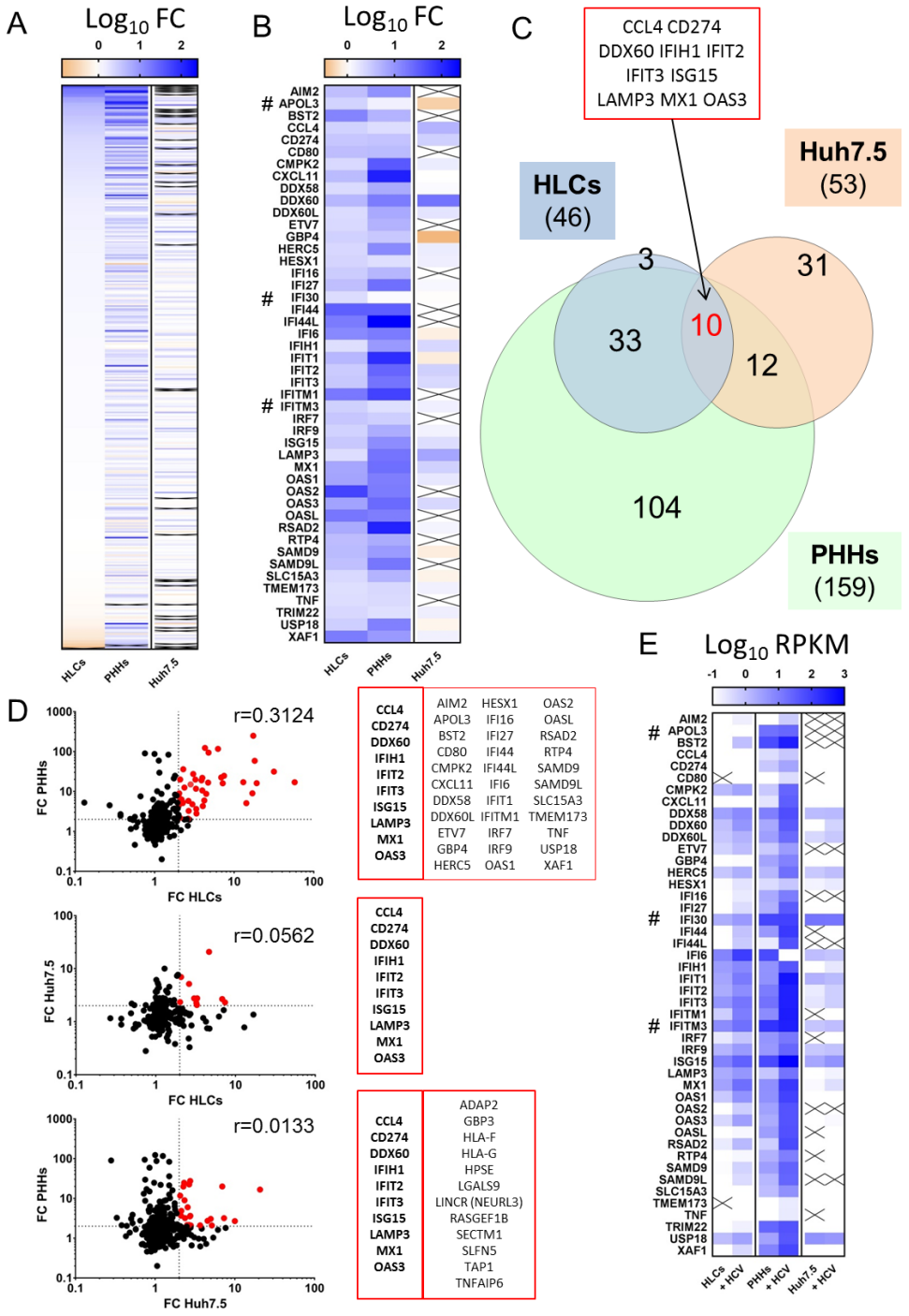

Figure 4 Interferon-regulated genes (IRGs) expression in stem cell-derived hepatocyte-like cells (HLCs) vs primary human hepatocytes (PHHs) vs Huh-7.5 and their induction by HCV infection (online supplementary table S4). PHHs and Huh-7.5 cells were inoculated with HCV Jc1 at an MOI 1, respectively. Cells were collected at 72 hours after inoculation and subjected to transcriptomic profiling. (A, B) Fold change on HCV infection of the 417 studied IRGs in HLCs, PHHs and Huh-7.5, ranked based on their overexpression in HCV-infected HLCs. Panel B illustrates the 46 IRGs upregulated more than twofold in HLCs (online supplementary table S5). # indicates the three IRGs upregulated in HLCs but not in PHHs. (C) Venn diagram of IRGs overexpressed in infected HLCs, Huh-7.5 and PHHs. (D) Correlation of expression fold change on HCV infection between HLCs, PHHs or Huh-7.5. Dotted line indicates fold change of 2. Red dots are IRGs upregulated in both cell models and are listed in the adjacent table. Pearson's correlation coefficient r is displayed. (E) Average Reads Per Kilobase of transcript, per Million mapped reads (RPKM) values for IRGs upregulated more than twofold in infected HLCs and their respective expression in Huh-7.5 and PHHs, control or infected.

specifically blocked induction of IFNs and IRGs upon triggering of RLR (online supplementary figure S4). Finally, blocking IFNAR-dependent signalling, or silencing of STAT1 expression enhanced infection (figure 2). These data emphasise the role of IFNs in control of HCV infection of HLCs and support the conclusion that ruxolitinib enhances HCV infection by blocking JAK/STAT signalling.

Time-dependent administration of ruxolitinib provided several interesting insights. When added concomitant with virus inoculation, kinetics of infectious virus accumulation

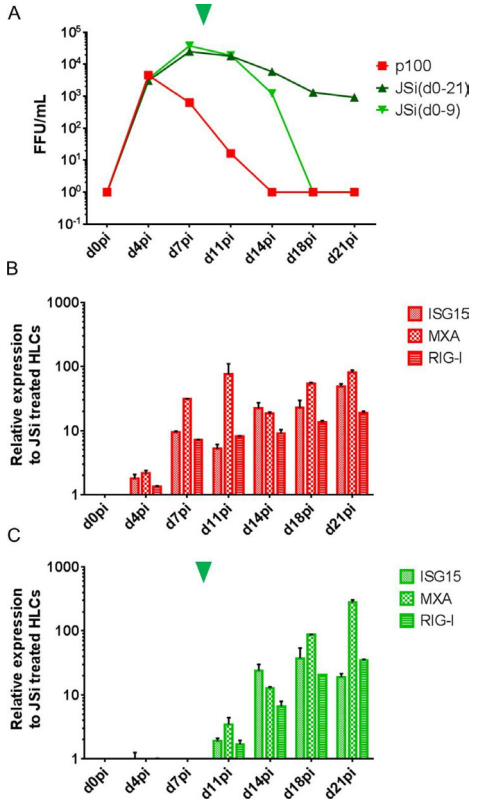

Figure 5 Chronic stem cell-derived hepatocyte-like cell (HLC) infection by HCV p100 and its JAK/STAT-dependent clearance. A representative experiment of three is given. (A) Production of infectious progeny virions by HLCs infected with HCV p100 (MOI: 0.5), cultured for 21 days in absence (red) or presence of ruxolitinib (JAK/STATpathway inhibitor (JSi)) from d0pi to d21pi (dark green) or from only d0pi to d9pi (light green, arrowhead indicates time of withdrawal of JSi). Expression of selected interferon-regulated genes (IRGs) (B) in infected, non-treated HLCs, and (C) in infected HLCs treated with ruxolitinib from d0pi to d9pi, normalised to infected, ruxolitinib-treated HLCs, assessed by RT-qPCR.

were very similar in the presence or absence of the drug for the first days of infection, with some minor fluctuation between experiments observed (figures 1A, 5A, online supplementary figures S5 and S6). These data suggest that, during this time period, HCV efficiently escapes or does not trigger JAK/STAT-signalling-dependent innate immune defenses. In line with this notion, highly sensitive RT-qPCR analysis of HCV-infected HLCs revealed only minimal IFN and IRG mRNAs induction until d4pi, despite of readily detectable de novo infectious virus production. We cannot completely rule out that HCV infection is sensed immediately after infection but in too few cells (as illustrated by fluorescence microscopy, figure 1E and online supplementary figure S5D) to be detected by our assays.

Clearly, during virus transmission in vivo, HCV frequently overcomes these liver intrinsic innate restrictions and establishes a chronic infection. In the HLC-p100 model, infection is typically cleared between day 11 and 14 after inoculation, unless pharmacological ablation of IRG induction. This difference could relate to distinct HCV replication levels, and different robustness of innate immune responses between HLCs ex vivo and hepatocytes in vivo. Nevertheless, this novel HCV-HLC infection model provides unique opportunities to dissect the importance of IFN-dependent and IFN-independent mechanisms of HCV control on natural HCV infection and with endogenously expressed viral sensors and effectors. The innate immune response mounted during the second week pi closely mirrors the one observed on HCV Jc1 infection of PHHs. While the induction of the anti-HCV innate immunity in infected HLCs seemed quantitatively lower than the one in infected PHHs, detailed comparative pathway analysis showed that the responses in HLCs and PHHs are qualitatively similar (online supplementary table S3). It confirms the authenticity of HLCs as an in vitro model for studying the hepatocyte reaction to HCV infection.

While working with PHHs presents strong technical limitations, working with hPSCs could hold the key to better experimental approaches. For example, hPSCs can be genetically engineered using CRISPR/Cas9 and subsequently differentiated in HLCs reproducing the edited phenotype.[37] Moreover, hiPSCs can be derived from patients with interesting genetic background, for example, polymorphisms in the type III IFNs genes, associated with spontaneous clearance and response to treatments.[38] While this strategy has been proposed,[11] it has not been so far used to decipher patient-specific innate immune response on in vitro HCV infection. We sequenced our hPSCs for single nucleotide polymorphisms of interest (online supplementary figure S12). Interestingly, H9ESC are homologous for the rs368234815(TT/ΔG) non-favourable ΔG allele, which leads to the expression of IFNL4, and is in patients associated with higher IRGs induction.[39] Future studies involving p100, which robustly infects HLCs, and tailored ESC or iPSC cells representing these and other loci may help to discover new principles that govern the highly variable courses and outcomes of HCV infection, thereby instructing personalised infection medicine.

Acknowledgements The authors would like to thank Dr KG Chen and Dr TJ Liang (NIH, USA) for the generation and transfer of the H9ESC adapted to monolayer culture; Professor CM Rice (Rockefeller University, USA) for the Huh-7.5 cells and the 9E10 anti-NS5A antibody; Professor E Domingo (Center for Molecular Biology 'Severo Ochoa', Spain) for the p100 HCV population; Michael Engelmann, Dr Gisa Gerold and the HZI Genome Analytics research centre for technical support.

Contributors AC and TP designed the study concept, analysed data and wrote the manuscript. AC also performed experiments. JS and RB performed experiments, analysed data and edited the manuscript. FWRV provided essential reagents and edited the manuscript.

Funding This study is funded by the Deutsche Forschungsgemeinschaft (DFG, German Research Foundation)—Project ID 158989968—SFB900, subprojects A6 and under the Germany's Excellence Strategy—EXC 2155 'RESIST'—Project ID 39087428.

Disclaimer The funders had no role in study design, data collection and analysis, decision to publish or preparation of the manuscript.

Competing interests None declared.

Patient and public involvement Patients and/or the public were not involved in the design, conduct, reporting or dissemination plans of this research.

Patient consent for publication Not required.

Provenance and peer review Not commissioned; externally peer reviewed.

Data availability statement Data are available upon reasonable request to: Dr Arnaud Carpentier, arnaud.carpentier@twincore.de, ORCID identifier 0000-0002-6994-4689; Professor Thomas Pietschmann, thomas.pietschmann@twincore.de, ORCID identifier 0000-0001-6789-4422.RNA-seq data are publicly available through the NIH GEO platform (https://www.ncbi.nlm.nih.gov/geo/): GEO accession GSE132606 and GSE132548.

ORCID iD
Arnaud Carpentier http://orcid.org/0000-0002-6994-4689

REFERENCES

1 World Health Organization. Global hepatitis report 2017.
2 Hill AM, Nath S, Simmons B. The road to elimination of hepatitis C: analysis of cures versus new infections in 91 countries. *J Virus Erad* 2017;3:117–23.
3 Sumpter R, Loo Y-M, Foy E, *et al*. Regulating intracellular antiviral defense and permissiveness to hepatitis C virus RNA replication through a cellular RNA helicase, RIG-I. *J Virol* 2005;79:2689–99.
4 Podevin P, Carpentier A, Pène V, *et al*. Production of infectious hepatitis C virus in primary cultures of human adult hepatocytes. *Gastroenterology* 2010;139:1355–64.
5 Thomas E, Gonzalez VD, Li Q, *et al*. HCV infection induces a unique hepatic innate immune response associated with robust production of type III interferons. *Gastroenterology* 2012;142:978–88.
6 Park H, Serti E, Eke O, *et al*. IL-29 is the dominant type III interferon produced by hepatocytes during acute hepatitis C virus infection. *Hepatology* 2012;56:2060–70.
7 Lucendo-Villarin B, Rashidi H, Cameron K, *et al*. Pluripotent stem cell derived hepatocytes: using materials to define cellular differentiation and tissue engineering. *J Mat Chem B* 2016;4:3433–42.
8 Shlomai A, Schwartz RE, Ramanan V, *et al*. Modeling host interactions with hepatitis B virus using primary and induced pluripotent stem cell-derived hepatocellular systems. *Proc Natl Acad Sci U S A* 2014;111:12193–8.
9 Xia Y, Carpentier A, Cheng X, *et al*. Human stem cell-derived hepatocytes as a model for hepatitis B virus infection, spreading and virus-host interactions. *J Hepatol* 2017;66:494–503.
10 Wu X, Robotham JM, Lee E, *et al*. Productive hepatitis C virus infection of stem cell-derived hepatocytes reveals a critical transition to viral permissiveness during differentiation. *PLoS Pathog* 2012;8:e1002617.
11 Schwartz RE, Trehan K, Andrus L, *et al*. Modeling hepatitis C virus infection using human induced pluripotent stem cells. *Proc Natl Acad Sci U S A* 2012;109:2544–8.
12 Carpentier A, Tesfaye A, Chu V, *et al*. Engrafted human stem cell-derived hepatocytes establish an infectious HCV murine model. *J Clin Invest* 2014;124:4953–64.
13 Yan F, Wang Y, Zhang W, *et al*. Human embryonic stem cell-derived hepatoblasts are an optimal lineage stage for hepatitis C virus infection. *Hepatology* 2017;66:717–35.
14 Helsen N, Debing Y, Paeshuyse J, *et al*. Stem cell-derived hepatocytes: a novel model for hepatitis E virus replication. *J Hepatol* 2016;64:565–73.
15 Wakita T, Pietschmann T, Kato T, *et al*. Production of infectious hepatitis C virus in tissue culture from a cloned viral genome. *Nat Med* 2005;11:791–6.
16 Zhou X, Sun P, Lucendo-Villarin B, *et al*. Modulating innate immunity improves hepatitis C virus infection and replication in stem cell-derived hepatocytes. *Stem Cell Reports* 2014;3:204–14.
17 Sakurai F, Kunito T, Takayama K, *et al*. Hepatitis C virus-induced innate immune responses in human iPS cell-derived hepatocyte-like cells. *Virus Res* 2017;242:7–15.
18 Schöbel A, Rösch K, Herker E. Functional innate immunity restricts hepatitis C virus infection in induced pluripotent stem cell-derived hepatocytes. *Sci Rep* 2018;8:3893.
19 Li K, Foy E, Ferreon JC, *et al*. Immune evasion by hepatitis C virus NS3/4A protease-mediated cleavage of the Toll-like receptor 3 adaptor protein TRIF. *Proc Natl Acad Sci U S A* 2005;102:2992–7.
20 Kato H, Takeuchi O, Sato S, *et al*. Differential roles of MDA5 and RIG-I helicases in the recognition of RNA viruses. *Nature* 2006;441:101–5.
21 Saito T, Owen DM, Jiang F, *et al*. Innate immunity induced by composition-dependent RIG-I recognition of hepatitis C virus RNA. *Nature* 2008;454:523–7.
22 Wu B, Peisley A, Richards C, *et al*. Structural basis for dsRNA recognition, filament formation, and antiviral signal activation by MDA5. *Cell* 2013;152:276–89.
23 Cao X, Ding Q, Lu J, *et al*. MDA5 plays a critical role in interferon response during hepatitis C virus infection. *J Hepatol* 2015;62:771–8.
24 Metz P, Reuter A, Bender S, *et al*. Interferon-stimulated genes and their role in controlling hepatitis C virus. *J Hepatol* 2013;59:1331–41.
25 Wong M-T, Chen SS-L. Emerging roles of interferon-stimulated genes in the innate immune response to hepatitis C virus infection. *Cell Mol Immunol* 2016;13:11–35.
26 Schoggins JW, Wilson SJ, Panis M, *et al*. A diverse range of gene products are effectors of the type I interferon antiviral response. *Nature* 2011;472:481–5.
27 Kim M-J, Yoo J-Y. Inhibition of hepatitis C virus replication by IFN-mediated ISGylation of HCV-NS5A. *J Immunol* 2010;185:4311–8.
28 Itsui Y, Sakamoto N, Kurosaki M, *et al*. Expressional screening of interferon-stimulated genes for antiviral activity against hepatitis C virus replication. *J Viral Hepat* 2006;13:690–700.
29 Perales C, Beach NM, Gallego I, *et al*. Response of hepatitis C virus to long-term passage in the presence of alpha interferon: multiple mutations and a common phenotype. *J Virol* 2013;87:7593–607.
30 Sheldon J, Beach NM, Moreno E, *et al*. Increased replicative fitness can lead to decreased drug sensitivity of hepatitis C virus. *J Virol* 2014;88:12098–111.
31 Carpentier A, Nimgaonkar I, Chu V, *et al*. Hepatic differentiation of human pluripotent stem cells in miniaturized format suitable for high-throughput screen. *Stem Cell Res* 2016;16:640–50.
32 Arnaud N, Dabo S, Maillard P, *et al*. Hepatitis C virus controls interferon production through PKR activation. *PLoS One* 2010;5:e10575.
33 Arnaud N, Dabo S, Akazawa D, *et al*. Hepatitis C virus reveals a novel early control in acute immune response. *PLoS Pathog* 2011;7:e1002289.
34 Garaigorta U, Chisari FV. Hepatitis C virus blocks interferon effector function by inducing protein kinase R phosphorylation. *Cell Host Microbe* 2009;6:513–22.
35 Jammi NV, Whitby LR, Beal PA. Small molecule inhibitors of the RNA-dependent protein kinase. *Biochem Biophys Res Commun* 2003;308:50–7.
36 Gale MJ, Korth MJ, Tang NM, *et al*. Evidence that hepatitis C virus resistance to interferon is mediated through repression of the PKR protein kinase by the nonstructural 5A protein. *Virology* 1997;230:217–27.
37 Omer L, Hudson EA, Zheng S, *et al*. Crispr correction of a homozygous low-density lipoprotein receptor mutation in familial hypercholesterolemia induced pluripotent stem cells. *Hepatol Commun* 2017;1:886–98.
38 Dustin LB. Innate and adaptive immune responses in chronic HCV infection. *Curr Drug Targets* 2017;18:826–43.
39 Prokunina-Olsson L, Muchmore B, Tang W, *et al*. A variant upstream of IFNL3 (IL28B) creating a new interferon gene IFNL4 is associated with impaired clearance of hepatitis C virus. *Nat Genet* 2013;45:164–71.

Efficient acute and chronic infection of stem cell-derived hepatocytes by hepatitis C virus

Arnaud Carpentier[1]*, Julie Sheldon[1], Florian W. R. Vondran[2], Richard JP Brown[3], Thomas Pietschmann[1]*

[1]Institute of Experimental Virology, TWINCORE, Centre for Experimental and Clinical Infection Research; a joint venture between the Medical School Hannover (MHH) and the Helmholtz Centre for Infection Research (HZI), Hannover, Germany

[2]ReMediES, Department of General, Visceral and Transplant Surgery, Hannover Medical School, Hannover, Germany

[3]Division of Veterinary Medicine, Paul Ehrlich Institute, Langen 63225, Germany

*Correspondence to:

Arnaud Carpentier, Institute for Experimental Virology, Twincore, Feodor Lynen Strasse 7, 30625 Hannover, Germany; arnaud.carpentier@twincore.de

Tel: (+49) 0511-220027-133 Fax: (+49) 0511-220027-178

Thomas Pietschmann, Institute for Experimental Virology, Twincore, Hanover, , Feodor Lynen Strasse 7, 30625 Hannover, Germany; thomas.pietschmann@twincore.de

Tel: (+49) 0511-220027-130 Fax: (+49) 0511-220027-178

SUPPLEMENTARY MATERIAL & METHODS

Human Pluripotent Stem Cells and hepatic differentiation

H9 human Embryonic Stem Cells (H9 ESCs), also known as WA09, were obtained from WiCell Research Institute, and were previously adapted to monolayer culture by Dr. Kevin G Chen (NIH Stem Cell Unit).[s1] They were cultured and differentiated as we previously described.[s2] Briefly, H9 ESCs were cultured in mTeSR1 (Stem Cell Technologies) on 0.4 mg/mL of growth factor reduced (GF-) Matrigel (Corning), at 37 ^{o} C and 21% oxygen (figure S1A, D0). Before starting the hepatic differentiation, H9 ESCs were resuspended using Accutase and passed on 0.125 mg/mL of GF- Matrigel, in mTeSR1 containing 10µM of the RHO/ROCK Inhibitor Y-27632. The day after, H9 ESCs were differentiated into Definitive Endoderm (DE) over 4 days using the Definitive Endoderm STEMdiff^{TM} kit (Stem Cell Technologies) (figure S1A, D4). DE cells were then passaged 1 in 3 and cultured for 8 days on GF- Matrigel (0.125 mg/mL), in Differentiation medium (45% High glucose DMEM, 45% F12 supplement, 10% KOSR, 1 % NEAA, 1% Glutamine, 1% Penicillin Streptomycin) containing 1% DMSO and 100ng/mL of HGF in order to induce an hepatoblast-like phenotype (figure S1A, D12). Cells were then maturated for 3 days in Differentiation medium containing 1.10^-7M Dexamethasone, leading to so called Hepatocyte-like Cells (HLCs) resembling primary human hepatocytes (PHHs) (figure 1A, D15).

HLCs could be then maintained in culture for at least 3 weeks in Complete WEM medium, (William's E medium, 10% FCS, 1% Penicillin Streptomycin, 1µg/mL human Insulin, 5µg/mL Hydrocortisone 21-hemisuccinate, 1.8% DMSO) as described previously.[s2]

Use of H9 human embryonic stem cells for research purposes was licensed by the German Ethics Commission (AZ.3.04.02/0113A).

Primary human hepatocytes

Primary human hepatocytes (PHHs) were prepared as previously reported.[s3] Hepatocytes were isolated from donors subjected to partial hepatectomy and were obtained with written informed consent approved by the ethics commission of Hannover Medical School (Ethik-Kommission der MHH, #252-2008).

HCV infection

The HCV p100 population viral stock was a kind gift from Dr. E. Domingo (Center for Molecular Biology “Severo Orchoa”, Madrid, Spain). Jc1 and p100 adapted HCVcc were produced in Huh7.5 cells (a kind gift from Prof. C.M. Rice, Rockefeller University, New York City, USA) as described previously.[s4]

HLCs at Day 15 of differentiation were inoculated overnight with different M.O.I. of HCVcc Jc1 or p100, and then rinsed 3 times with PBS. Fresh Complete WEM medium was then added and changed every 2 to 3 days. To confirm the authenticity of HCV replication, some cells were cultured in presence of 10µM of the DAAs Telaprevir (a NS3-4A inhibitor) or Daclatasvir (a NS5B inhibitor) throughout the infection time course. To assess the effect of the innate immunity on HCV replication, HLCs were treated with 10µM of Ruxolitinib (AdipoGen Life Sciences, AG-CR1-3624), a JAK/STAT pathway inhibitor, for 16 hours before being inoculated with HCVcc. Infected cells were then maintained in medium containing 10µM Ruxolitinib, throughout the experiment.

HCV RNA RT-qPCR, IFA, Infectious Titer

Intracellular HCV RNA was quantified from isolated total cellular RNA using a quantitative, GAPDH duplexed, one step RT-qPCR protocol using the "Light Cycler 480 RNA Master Hydrolysis Probes" kit (Roche), and primers specific for the 5' UTR region of the JFH isolate (S: 5'-GGGCATAGAGTGGGTTTATCCA-3'; AS: 5'-TCTGCGGAACCGGTGAGTA-3'; Probe: 5'6FAM-AAAGGACCCAGTCTTCCCGGCAA-TMR) and GAPDH (S: 5'-GAAGGTGAAGGTCGGAGTC-3'; AS: 5'-GAAGATGGTGATGGGATTTC-3'; Probe: 5'-LC640-CAAGCTTCCCGTTCTCAGCCT-BBQ). RT-qPCR was performed on a LightCycler 480 (Roche), as follow: RT: 63°c, 3 min. Initial denaturation: 95°c, 30 sec. Amplification: 45 cycles of 95°c, 15 sec and 60°c, 30 sec. cooling: 40°c, 30 sec.

HCV infection of HLCs could be visualized using the 9E10 anti HCV NS5A monoclonal antibody, [s5] provided by Prof. C.M. Rice, diluted 1 in 1000 in PBS 1% BSA 0.1% Triton X100, on cells fixed in cold Methanol, permeabilized with 0.5% Triton X100, blocked with PBS 3%BSA, and visualized on a IX81 Olympus inverted microscope after DAPI counterstaining.

Infectious titers were measured in supernatant of inoculated cells, by incubating Huh7.5 cells for 3 days with serial dilution of supernatant in complete DMEM medium. Huh7.5 cells were then fixed with cold methanol, permeabilized with 0.5% Triton X100, blocked with PBS 3% BSA, and infected foci visualized using the 9E10 anti NS5A antibody as explained above.

Immunostaining & ELISA

For immunostaining of differentiation markers assessed via fluorescent microscopy, uninfected cells were fixed using 3% PFA, permeabilized using 0.5% Triton X100 dissolved in PBS, and blocked using PBS 3% BSA. The switched expression from pluripotency marker to DE cells

markers was validated by simultaneously staining for OCT4 (Santa Cruz, sc-9081, 1:400), SOX17 (R&D, AF1924, 1:100) and FOXA2 expression (Santa Cruz, sc-271103, 1:100). Hepatoblasts and HLCs were tested for HNF4A (Santa Cruz, sc-6556, 1:100), AFP (Sigma Aldrich, A8452, 1:330), and albumin (Cedarlane, CL2513A, 1:330). Expression of the IRGs ISG15 (Santa Cruz, sc-323987, 1:100), IFIT1 (Santa Cruz, sc-134948, 1:100) and IRF3 (Cell Signaling, #11904, 1:400) were also assessed by immunofluorescent assay (IFA) on HLCs, with the only difference than infected HLCs were first fixed with Cold Methanol instead of 3% PFA. All antibody incubations were performed in PBS 0.1% Triton X100 1% BSA, and cells were counterstained with DAPI (1/10000) before image acquisition on a IX81 Olympus inverted microscope

Albumin secretion was quantified in supernatants using the Human Albumin ELISA Quantitation Set (Bethyl Laboratories, E80-129). Production of lipoproteins by HLCs were assessed by measuring secretion of the apolipoproteins ApoB (Mabtech, 3715-1A-20) and ApoE (Mabtech, 3712-1H-20) in the supernatant of HLCs. ELISA assays were performed according to the manufacturer's instruction.

CYP3A4 metabolic assay

CYP3A4 activity in HLCs was assessed using the Luciferin-IPA P450-Glo Assay (Promega), an assay only moderately affected by the DMSO present in the WEM HLCs culture medium, following the manufacturer's instructions. Briefly, cells were incubated at 37°c for 1 or 2 hours with 3µM of the Luciferin-IPA CYP3A4 substrate. Luciferin produced by conversion of the substrate by the CYP450 was then measured in the culture medium.

Innate immunity induction by IFNα and Poly IC

HLCs were treated for 24 hours with 1000 IU/mL of IFNα2b. For poly(I:C) stimulation, cells were incubated for 24 hours with 1µg/mL of poly(I:C), with or without prior mixing with lipofectamine 2000 (2µl Lipofectamine 2000 per 1µg Poly(I:C), 15 minutes at RT in OptiMEM). After 24h, cells were lysed and total RNAs were isolated according to the manufacturer's instructions using the NucleoSpin RNA kit (Macherey-Nagel). Supernatants were collected for IFN bioactivity assay.

RT-qPCR

Total cellular RNA was isolated according to manufacturer's instructions using the NucleoSpin RNA kit (Macherey-Nagel). 200 ng of total RNA was then reverse transcribed using the Takara Reverse Transcription (RT) kit. 100ng of cDNA per reaction were used for quantification using Takara's SYBR Premix Ex Taq II according to the manufacturers' instructions. Samples were then run on a Light Cycler 480 (Roche). Relative expression was calculated following the $2^{-\Delta\Delta CT}$ methods, as described in Livak et al.[s6] Primers used in our study:

IFNα	S	GCTTTACTGATGGTCCTGGTGGTG
	AS	GAGATTCTGCTCATTTGTGCCAG
IFNβ	S	ATGACCAACAAGTGTCTCCTCC
	AS	GGAATCCAAGCAAGTTGTAGCTC
IFNλ2-3 IL28	S	CTTTAAGAGGGCCAAAGATGC
	AS	CCAGCTCAGCCTCCAAAG
IFNλ1 IL29	S	TTCCAAGCCCACCACAAC
	AS	TCCCTCACCTGGAGAAGC
ISG15	S	CGCAGATCACCCAGAAGATCG
	AS	TTCGTCGCATTTGTCCACCA
MAVS	S	CAGGCCGAGCCTATCATCTG
	AS	GGGCTTTGAGCTAGTTGGCA
MDA5	S	TCGAATGGGTATTCCACAGACG
	AS	GTGGCGACTGTCCTCTGAA

MXA	S	GTTTCCGAAGTGGACATCGCA
	AS	CTGCACAGGTTGTTCTCAGC
RIG-I	S	CTGGACCCTACCTACATCCTG
	AS	GGCATCCAAAAAGCCACGG
AFP	S	GCAGCCAAAGTGAAGAGG
	AS	TGTTGCTGCCTTTGTTTG
ALB	S	GGCACAATGAAGTGGGTAAC
	AS	AGGCAATCAACACCAAGG
CYP3A4	S	CCTTACATATACACACCCTTTG
	AS	GGTTGAAGAAGTCCTCCTAAGCT
GAPDH	S	GAAGGTGAAGGTCGGAGTC
	AS	GAAGATGGTGATGGGATTTC

IFN bioactivity assay

The secreted type I and III IFN bioactivity was quantified by incubating the reporter cell line HL116 that carries the luciferase gene under the control of the IFN-inducible 6-16 promoter[s7] with diluted supernatant of HLCs. A standard curve was calculated using serial dilution of IFNα2b (Roferon) to transform reporter signals to international units of IFN activity.

siRNA and IFNAR neutralization assay

siRNA against human STAT1 and STAT2 were obtained from Ambion. One day before infection, HLCs were transfected with 3µl RNAi MAX Lipofectamine and 20pmol of siRNA (40µM final) per well of a 24 well plate, following the manufacturer's instructions. Transfection was then repeated on infected cells at day 2, 4 and 7pi.

Target	Ambion ID	Sequence
Human STAT1	s279	UCCGCAACUAUAGUGAACCdAdG
Human STAT2	s13528	UUAGAGACCACAAUGAGCCdTdG

The day before HCV inoculation, HLCs were incubated with 5, 10 and 20 µg/ml of Mouse Mab against human IFN Alpha/Beta Receptor (PBL Assay Science, 21385-1). After adding HCV input overnight, cells were rinsed and new Complete WEM medium was added without neutralizing Ab.

RNA-seq and pathway analyses

Transcriptomic analyses were performed in duplicate or triplicate. Total cellular RNA quality assessment was achieved using an Agilent Bioanalyser and 500ng were used to generate a RNA sequencing library with ScriptSeq v2 RNA-Seq Library Preparation Kit (Epicentre, Illumina). The sequencing was performed on an Illumina HiSeq2500 machine (Illumina). Transcriptomic analyses were performed using CLC Genomics Workbench (Qiagen, Aarhaus). Generated Fastq files were mapped against the hg19 human reference genome with annotated gene and mRNA tracks. Gene expression was calculated for individual transcripts as reads per kilobase per million bases mapped (RPKM). When rank ordering cellular gene expression profiles, mitochondrially encoded transcripts were omitted from the analyses.

All raw and processed files can be found online at https://www.ncbi.nlm.nih.gov/geo/, using the GEO accession code GSE132606 for SC and HLCs related RNA-seq and GSE132548 for Huh-7.5 and PHHs related works. Pathway enrichment analyses were performed on the list of the top 1000 most upregulated genes compared to non-infected cells, using STRING v11 (https://string-db.org/),[s8] and the Gene Ontology (GO) Enrichment Analysis tool (http://geneontology.org/).[s9,s10]

Type III IFN SNPs sequencing

Genomic DNA was isolated from H9ESC using the DNeasy Blood & Tissue Kit (Qiagen), following the manufacturer's instructions. Specific portions of the *IL28B* gene carrying SNPs of interest were amplified using 0.5µM of specific primers (see table below) and the Hot Start Taq Polymerase kit (Qiagen) following the manufacturer's instructions. PCR Run was performed 0n a T100 Thermocycler (Biorad) as follow: 15 min at 95°c; 40 cycles of 30 sec at 95°c, 30 sec at specific annealing temperature (see table below), 30 sec at 72°c; 10 min at 72°c. Amplification was confirmed on a 1% agarose gel, and genotypes determined by Sanger sequencing.

rs12979860	S AS	GATTCCTGGACGTGGATG GCTCAGGGTCAATCACAGAAG	Annealing temperature 58°c
rs8099917	S AS	TCACCATCCTCCTCTCATCC TGCTGGGCCCTAACTGATAC	Annealing temperature 60°c
rs368234815	S AS	GTGCCTTCACGCTCCGAGCA TCCCTCAGCGCCTTGGCA	Annealing temperature 62°c
rs117648444	S AS	GCTCAGGGTCAATCACAGAAG GGACGAGAGGGCGTTAGAG	Annealing temperature 60°c

Statistics

Statistical analyses were performed in Microsoft Excel 2010 and GraphPad Prism software. *In vitro* data are expressed as average of 3 to 5 independent experiments, and 2-tailed Student's t-test or 2-way ANOVA were performed to assess statistical significance. A p-value <0.05 was considered significant (*), a p-value <0.01 highly significant (**). Correlation was evaluated using Pearson correlation coefficient. Pathway analysis p-values were calculated with Bonferroni correction.

SUPPLEMENTARY FIGURES

Figure S1: Hepatic differentiation of human pluripotent stem cells. (A) Differentiation protocol of H9 ESC (SC) into Definitive Endoderm (DE), Hepatoblasts (Hep) and finally Hepatocyte-like Cells (HLCs) and their phenotypic characterization by contrast phase and fluorescent microscopy at the different stages of differentiation, compared to primary culture of adult hepatocytes (PHHs). (B) ELISA for human ALB secreted at different steps of differentiation and maintenance of HLCs. Means of >10 biological replicates and standard deviation are shown. (C-E) RNA-seq analysis throughout differentiation of: (C) pluripotency markers, (D) definitive endoderm associated genes and (E) hepatocyte associated genes compared to PHHs and Huh7.5. A RPKM value of 0.5 is considered a threshold for tissue specific gene expression. Crosses represent genes not detected by RNA-seq. RNA-seq data repository available with GEO accession code GSE132606.

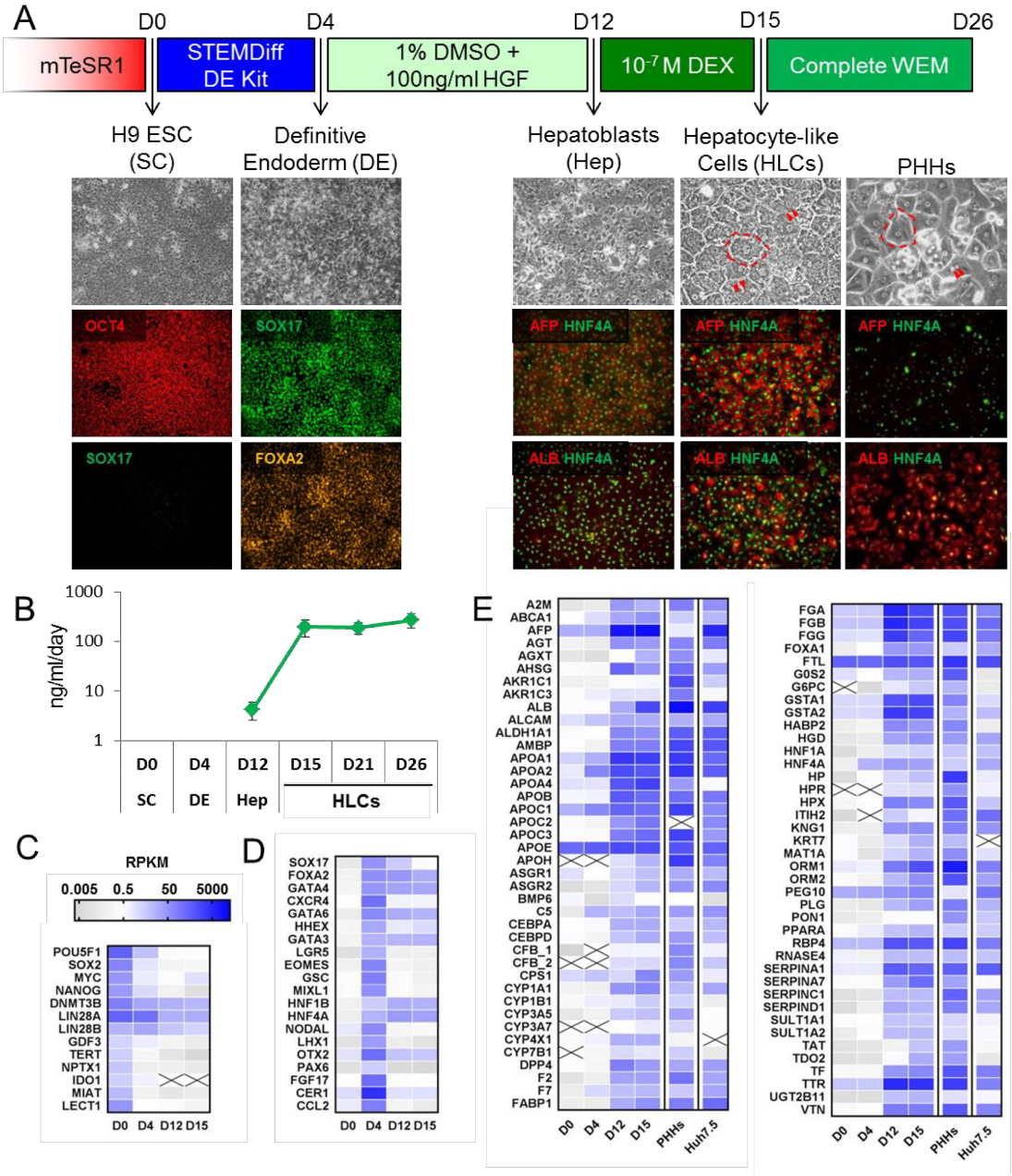
A
D0
D4
D12
D15
D26
mTeSR1
STEMDiff DE Kit
1% DMSO + 100ng/ml HGF
10-7 M DEX
Complete WEM
H9 ESC (SC)
Definitive Endoderm (DE)
Hepatoblasts (Hep)
Hepatocyte-like Cells (HLCs)
PHHs
OCT4
SOX17
AFP HNF4A
ALB HNF4A
FOXA2
B
ng/ml/day
1000
100
10
1
D0 D4 D12 D15 D21 D26
SC DE Hep HLCs
C
RPKM
0.005 0.5 50 5000
POU5F1
SOX2
MYC
NANOG
DNMT3B
LIN28A
LIN28B
GDF3
TERT
NPTX1
IDO1
MIAT
LECT1
D0 D4 D12 D15
D
SOX17
FOXA2
GATA4
CXCR4
GATA6
HHEX
GATA3
LGR5
EOMES
GSC
MIXL1
HNF1B
HNF4A
NODAL
LHX1
OTX2
PAX6
FGF17
CER1
CCL2
D0 D4 D12 D15
E
A2M
ABCA1
AFP
AGT
AGXT
AHSG
AKR1C1
AKR1C3
ALB
ALCAM
ALDH1A1
AMBP
APOA1
APOA2
APOA4
APOB
APOC1
APOC2
APOC3
APOE
APOH
ASGR1
ASGR2
BMP6
C5
CEBPA
CEBPD
CFB_1
CFB_2
CPS1
CYP1A1
CYP1B1
CYP3A5
CYP3A7
CYP4X1
CYP7B1
DPP4
F2
F7
FABP1
D0 D4 D12 D15 PHHs Huh7.5
FGA
FGB
FGG
FOXA1
FTL
G0S2
G6PC
GSTA1
GSTA2
HABP2
HGD
HNF1A
HNF4A
HP
HPR
HPX
ITIH2
KNG1
KRT7
MAT1A
ORM1
ORM2
PEG10
PLG
PON1
PPARA
RBP4
RNASE4
SERPINA1
SERPINA7
SERPINC1
SERPIND1
SULT1A1
SULT1A2
TAT
TDO2
TF
TTR
UGT2B11
VTN
D0 D4 D12 D15 PHHs Huh7.5

Figure S2: Immunofluorescence and RNA-seq monitoring of hepatic differentiation. (A) Immunostaining and (B) RPKM values for pluripotency marker POU5F1/OCT4, definitive endoderm markers SOX17 and FOXA2, and hepatic markers AFP, HNF4A and ALB at different stages of differentiation compared to PHHs show correlation between RNA-seq and protein expression. (C) Top 28 expressed transcripts in HLCs after 6 days of maturation in WEM medium (D21) and their respective expression of ranking in PHHs confirm strong hepatic phenotype of the HLCs. Green highlights indicate genes specifically associated with hepatocytes metabolism. (D) RPKM ranking of HLC expressed transcripts at the time of HCV infection, highlighting selected hepatic markers and HCV entry factors, confirms the *a priori* permissiveness of HLCs to HCV. (E) RPKM analysis for endodermal pancreatic markers (grey means below the threshold of RPKM=0.5 above which a gene is considered tissue specific; crosses indicate no transcript mRNA detected) throughout differentiation compared to hepatic markers AFP, HNF4A and ALB (color) confirms the specificity of our hepatic differentiation protocol.

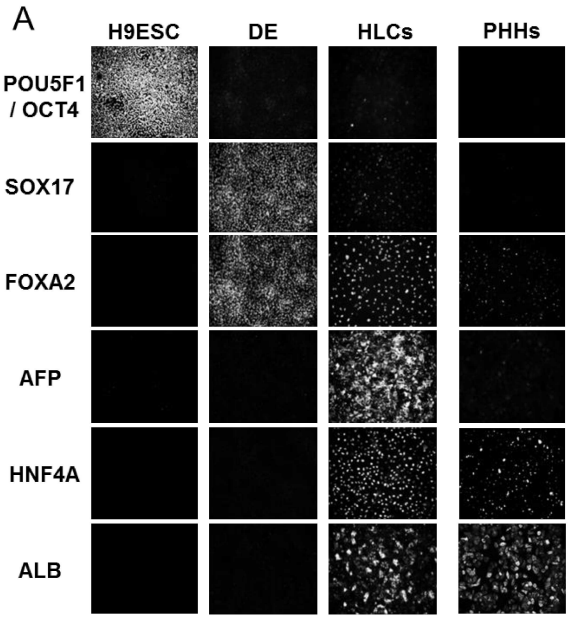

C

Rank	Name	H9ESC	DE	HLCs	PHHs	Rank in PHHs
1	AFP	16.67	16.21	20044.52	1.18	10012
2	FGB	6.22	5.84	5741.32	1052.54	30
3	TTR	5.26	5.20	4646.81	2118.83	12
4	APOA1	3.50	15.59	3986.01	2410.48	9
5	FTL	422.74	331.57	3237.79	3085.45	6
6	APOA4	1.89	1.75	3128.37	36.88	1381
7	GSTA1	2.69	2.51	3124.15	97.60	483
8	GSTA2	2.83	2.77	2529.02	13.53	3340
9	FGG	2.17	1.85	2439.65	1476.23	20
10	SERPINA1	1.31	1.20	2121.62	497.11	87
11	ORM1	1.36	0.98	1567.80	9509.50	2
12	APOC3	0.59	0.58	1498.49	1764.51	18
13	APOA2	1.25	95.16	1445.69	2818.66	7
14	TMSB10	1658.93	4498.97	1382.30	1959.10	14
15	APOE	312.84	540.33	1143.32	862.18	41
16	RBP4	9.50	9.66	906.75	1641.68	19
17	APOB	0.71	0.87	848.26	280.56	144
18	GPC3	38.17	6.86	838.32	0.03	16407
19	FTH1	660.58	842.26	837.59	2095.22	13
20	ACTB	575.31	757.60	823.80	3185.72	5
21	PRDX1	380.77	348.03	786.66	205.20	211
22	SERPINA7	0.28	0.29	668.87	27.04	1857
23	PEG10	18.43	24.45	591.12	1.55	9354
24	EEF1A1	1203.16	870.00	577.49	1185.35	24
25	TF	0.25	0.18	542.60	739.05	51
26	S100A14	0.96	45.23	523.51	139.68	324
27	ALB	0.53	0.62	514.15	18282.23	1
28	ACTG1	541.87	730.80	508.07	516.04	81

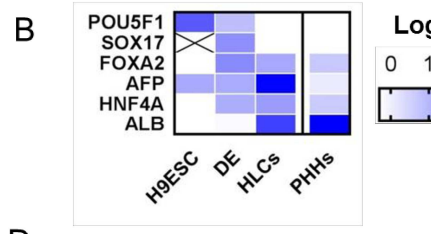

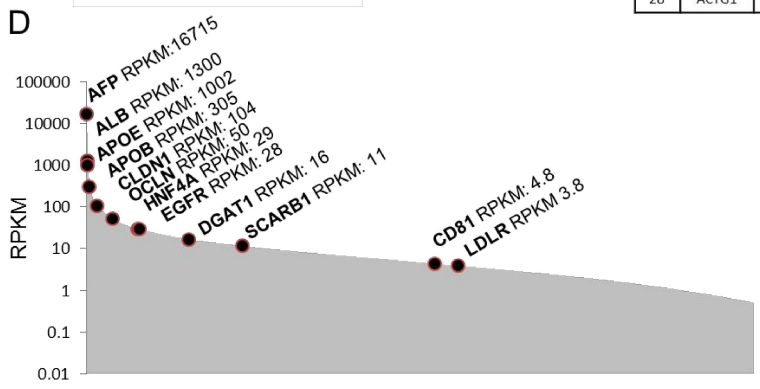

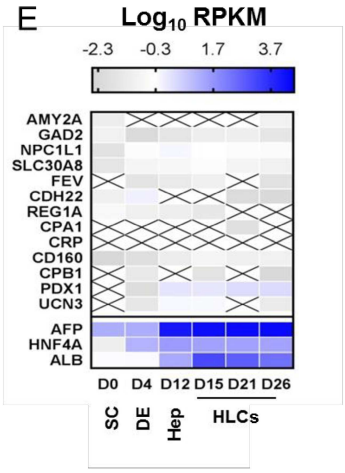

Figure S3: Transcriptional profiling of innate immune genes in the course of stem cell differentiation. (A) Expression of innate immune genes changes during differentiation from a subset of IRGs (i.e. BST2 and IFITMs) to a low, IFN-inducible system based on expression of PRRs, as described previously.[s11] (B) In HLCs, key viral PRRs, IFN receptors, and genes involved in the IFN pathway were expressed at similar level to PHHs, with the notable exception of TLR3, expressed only at very low levels in HLCs. Huh-7.5 cells also do not express detectable level of TLR3, and display lower level of expression of certain IRGs.

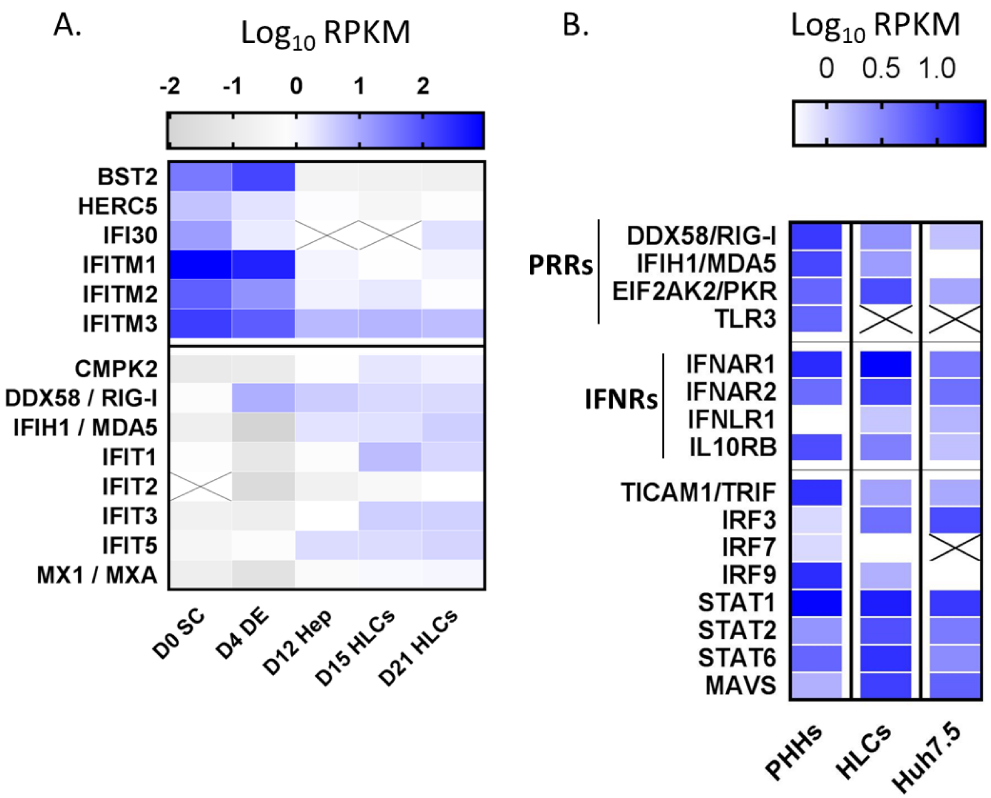

Figure S4: Characterization of innate immunity in HLCs. HLCs were incubated for 24 h with (Poly(I:C)) or transfected with Poly(I:C) (Lipofectamine), treated with 1,000 IU/mL IFNα2B, or left untreated (Ctrl). (A) Cells were fixed and stained with an IRF3-specific antibody (red), revealing nuclear translocation of IRF3 only after Poly(I:C) transfection. Nuclear DNA was counterstained with DAPI (blue). (B) Total RNA was extracted, and mRNA expression of IFNs was examined by qRT-PCR and expressed relative to the GAPDH mRNA. Type I and III IFNs were significantly up-regulated upon Poly(I:C) transfection, with IFN-λs being expressed at a higher level than IFN-α and -β, suggesting that they are the main IFNs expressed by HLCs upon PRRs triggering. (C) Secretion of IFNs was monitored by using an IFN-responsive reporter cell line. (D) HLCs were mock-treated or supplemented with 1000IU/mL IFNα2B, Poly(I:C) or Lipofectamine + Poly(I:C), in the presence or absence of Ruxolitinib (JSi). 24h later, total RNA of these cells was extracted, mRNA expression of selected genes was quantified and expressed as fold difference to mock treated cells. The IRGs RIG-I, MDA5, MXA and ISG15, but not the non-IRG MAVS were upregulated upon treatment with IFNα2B and upon transfection of Poly(I:C). For panel B-D, mean values of 3 replicates and the standard deviation are given. Statistics are calculated compared to ctrl cells. Statistical significance: *: $p < 0.05$; **: $p < 0.01$. (E) Immunostaining for IRGs ISG15 and IFIT1 (green) and hepatic markers (red) in untreated HLCs or HLCs treated with IFNα2B. Nuclear DNA was counterstained with DAPI (blue). Quantification of the mean fluorescent intensity (MFI) of the IRGs' staining is given. Statistical significance: *: $p < 0.05$; **: $p < 0.01$.

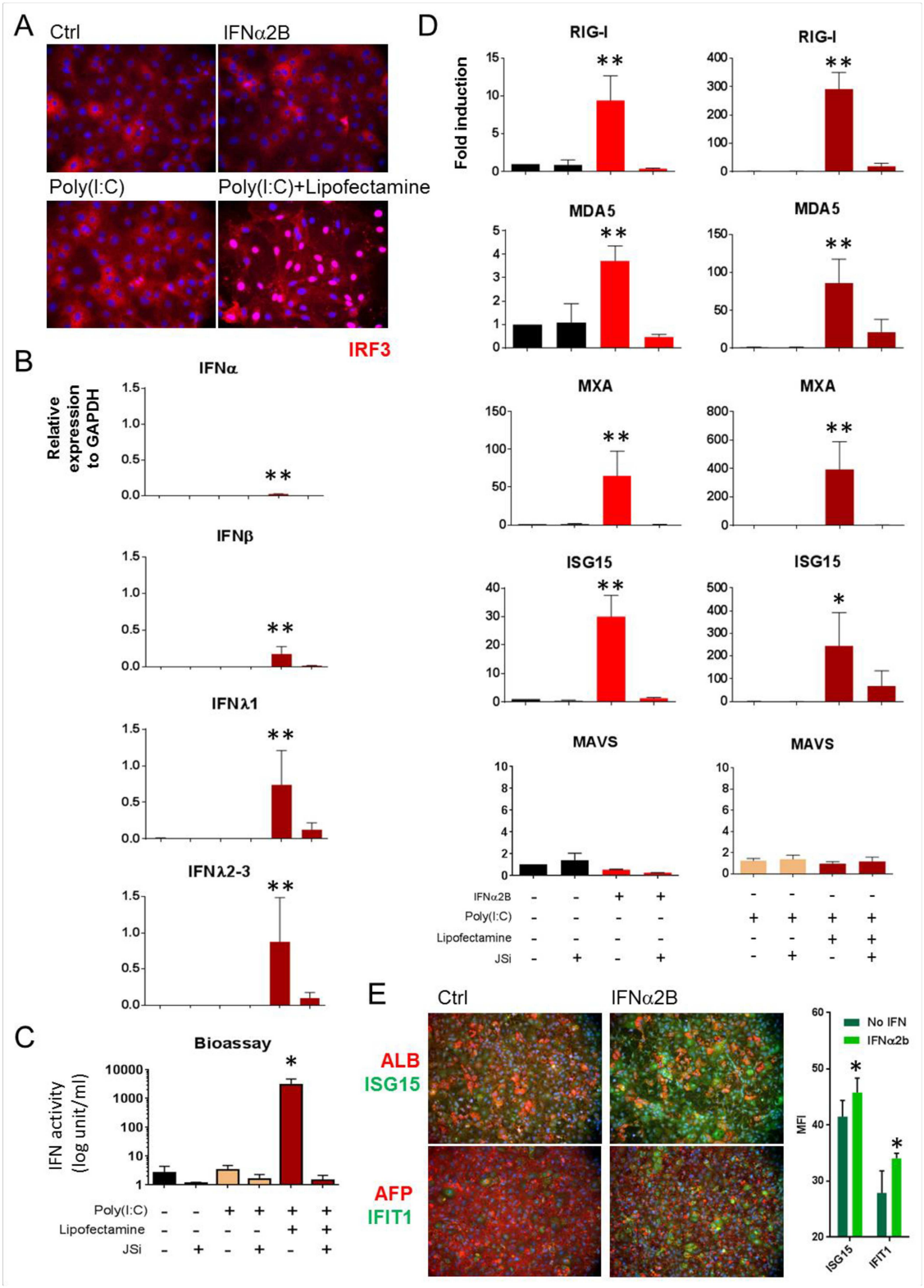
A
Ctrl
IFNα2B
Poly(I:C)
Poly(I:C)+Lipofectamine
IRF3
B
IFNα
IFNβ
IFNλ1
IFNλ2-3
Relative expression to GAPDH
C
Bioassay
IFN activity (log unit/ml)
Poly(I:C)
Lipofectamine
JSi
D
RIG-I
MDA5
MXA
ISG15
MAVS
Fold induction
IFNα2B
Poly(I:C)
Lipofectamine
JSi
E
Ctrl
IFNα2B
ALB
ISG15
AFP
IFIT1
No IFN
IFNα2b
MFI

Figure S5: Susceptibility of HLCs to the cell culture adapted p100 HCV virus population,[29-30] and its parent, the Gt2a chimera Jc1-HCVcc. HLCs were inoculated with Jc1 or p100 (MOI: 5 or 1, respectively). (A) Comparison of intracellular HCV RNA (quantified by qRT-PCR, left panel) and infectious virus production (right panel). Despite a lower MOI (MOI: 1 vs 5), p100 infection yielded ca. 50-fold greater intracellular RNA at 4 days post inoculation (dpi). Moreover, Jc1 infection yielded only very low infectious titers,[12] while p100 consistently reached peak infectious titers between 100 – 1,000-fold higher(10^3-10^4 FFU/mL) on d4pi. Mean values of 3 replicates and the standard deviation are given. (B) Treatment of p100-inoculated HLCs with 100µM of Telaprevir (DAA) or Ruxolitinib (JSi). Treatment with Telaprevir (blue) showed only a modest effect on intracellular p100 HCV RNA, possibly due to high stability of viral input RNA from the initial inoculum. In contrast, Telaprevir completely abrogated infectious virus production, confirming that infectious virus production depends on viral RNA replication and highlighting infectivity titration as a highly specific and quantitative readout for p100 infection of HLCs. Treatment with Ruxolitinib (green) led to 5 to 10-fold higher intracellular HCV RNA copy numbers within the 2^{nd} week pi, and allowed higher infectious titers, reaching up to 10^5 FFU/mL. (C) Ruxolitinib treatment only slightly enhanced Jc1 virus production in HLCs, but to level much lower than in p100 infected HLCs. (D) Visualization of p100 infected HLCs using the 9E10 monoclonal antibody against HCV NS5A. Ruxolitinib-treated HLCs also supported spreading of p100.

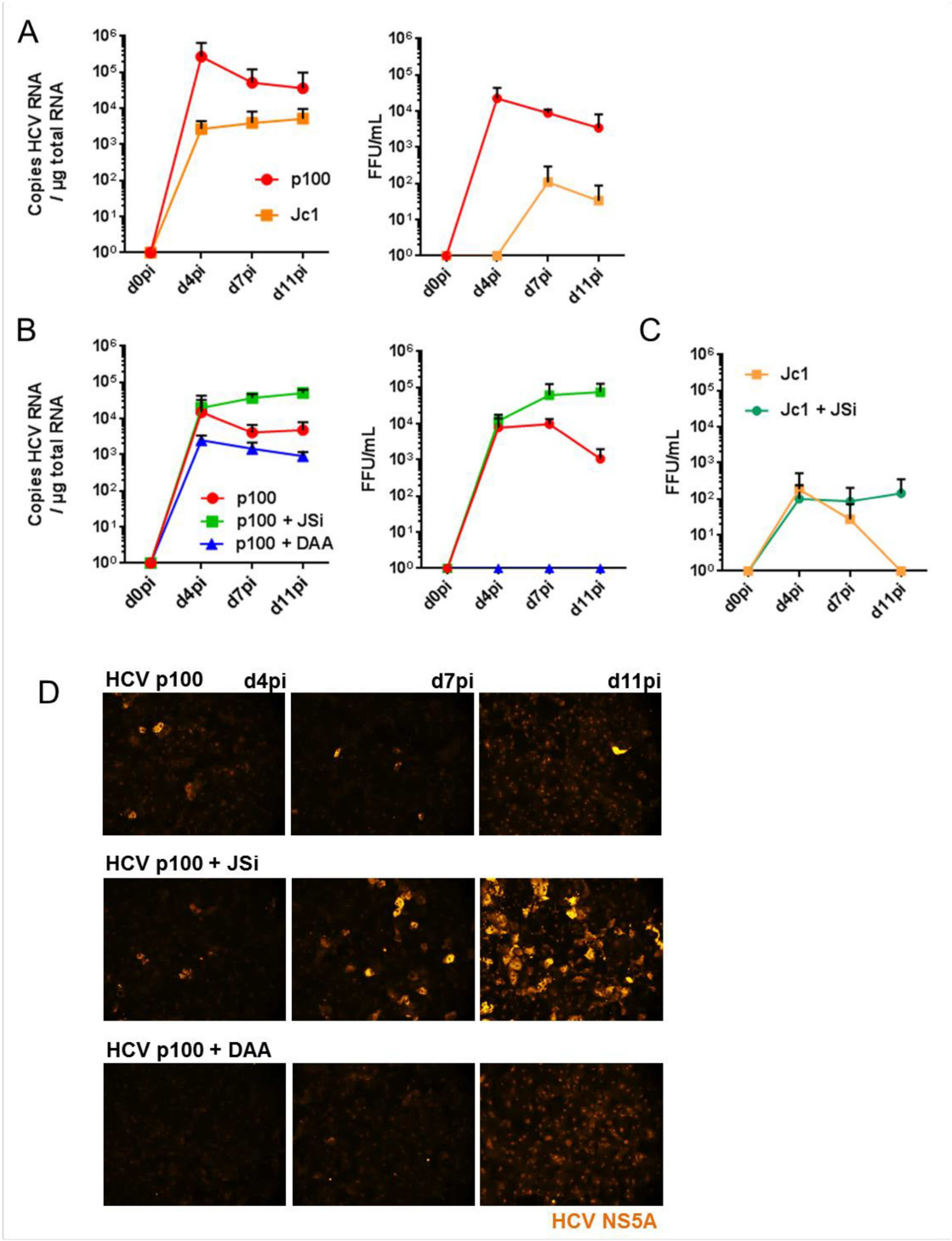
A
Copies HCV RNA / µg total RNA
FFU/mL
p100
Jc1
d0pi
d4pi
d7pi
d11pi
B
Copies HCV RNA / µg total RNA
FFU/mL
p100
p100 + JSi
p100 + DAA
C
FFU/mL
Jc1
Jc1 + JSi
D
HCV p100
d4pi
d7pi
d11pi
HCV p100 + JSi
HCV p100 + DAA
HCV NS5A

Figure S6: p100 HCV infection of HLCs. (A) DAAs abrogate effect of Ruxolitinib on HCV replication in HLCs. Intracellular HCV RNA quantification in HLCs infected with p100 HCVcc and treated with 10µM JSi and/or 10µM Telaprevir assessed by qRT-PCR. Quantification of intracellular HCV RNA in HCV infected, DAAs treated cells shows level of non-replicating HCV in the cells, suggesting that qRT-PCR is not a good readout method to assess permissivity of HLCs to HCV. (B) Infectious titer in supernatants of p100 HCVcc inoculated HLCs, treated with 10µM JSi, Telaprevir (TEL) and/or Daclatasvir (DAC), shows total inhibition of production of infectious progeny viruses upon treatment with DAAs. (C) IFIT1 protein expression upon HCV infection with or without JSi treatment. Quantification of the mean fluorescent intensity (MFI) of the IRGs' staining is given. Statistical significance: *: $p<0.05$; **: $p<0.01$.

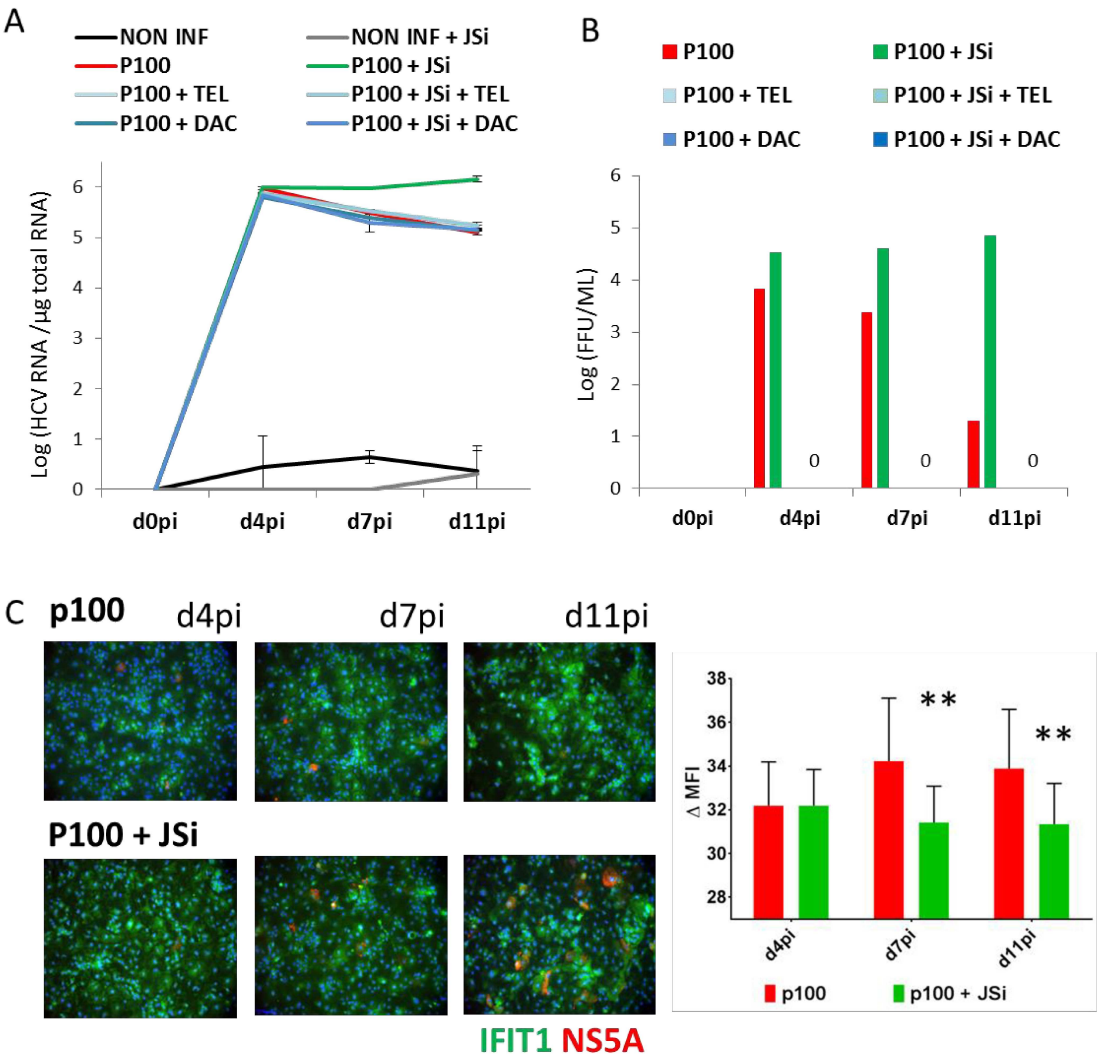
A
NON INF
NON INF + JSi
P100
P100 + JSi
P100 + TEL
P100 + JSi + TEL
P100 + DAC
P100 + JSi + DAC
Log (HCV RNA /µg total RNA)
d0pi
d4pi
d7pi
d11pi
B
P100
P100 + JSi
P100 + TEL
P100 + JSi + TEL
P100 + DAC
P100 + JSi + DAC
Log (FFU/ML)
C
p100
d4pi
d7pi
d11pi
P100 + JSi
IFIT1 NS5A
Δ MFI
**
**
p100
p100 + JSi

Figure S7: Effect of 10µM Ruxolitinib on gene expression in HLCs. HLCs were infected with HCV in presence (Jsi) or absence (HCV) of Ruxolitinib or were left untreated (Ctrl). On day 11 after inoculation, cells were subjected to transcriptional profiling. (A) Ruxolitinib does not alter the mRNA levels of canonical HCV host factors or (B) typical hepatic marker genes.

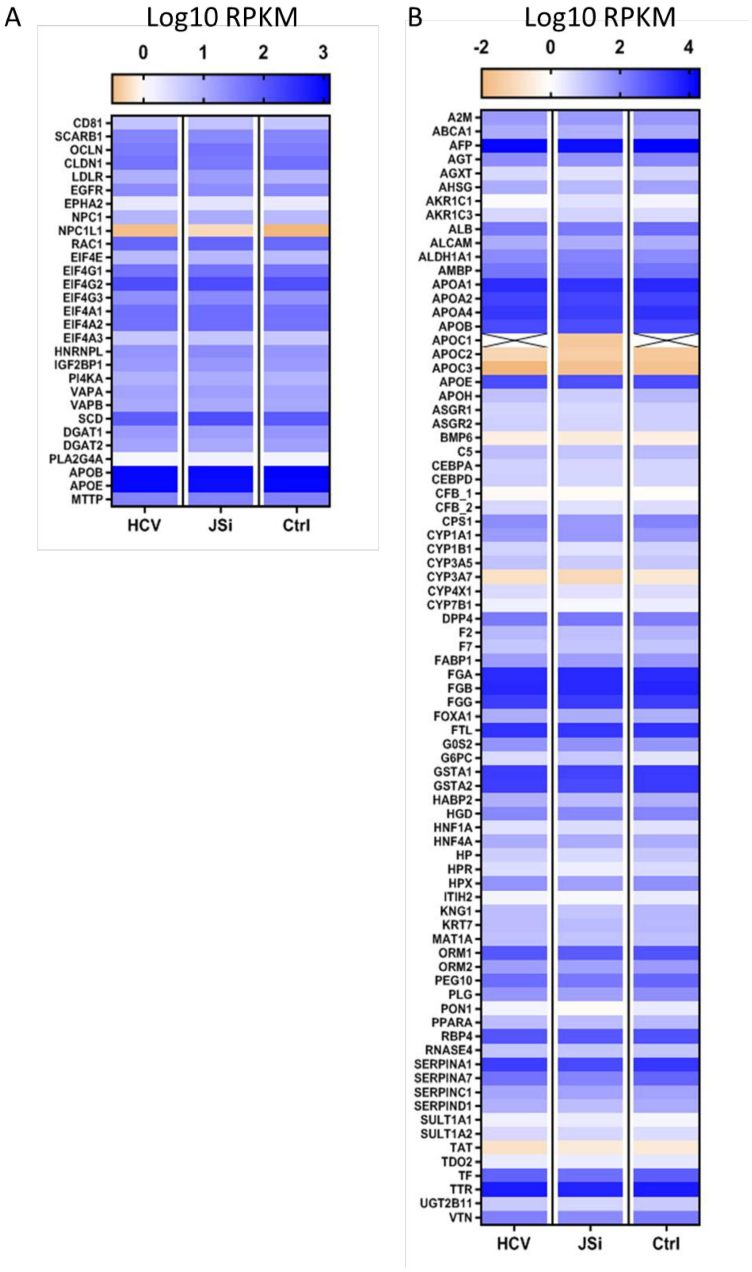

Figure S8: p100 HCV infection of primary human hepatocytes (PHH), in presence or absence of Ruxolitinib (JSi). PHHs were maintained for 6 days and maintenance of maturation was assessed by (A) contrast phase assesment and (B) albumin ELISA. (C) Upon inoculation with p100 HCV, production of infectious progeny viruses in the supernatant of PHHs. (D) Induction of IRGs in PHHs infected by p100 HCV, assessed by qPCR.

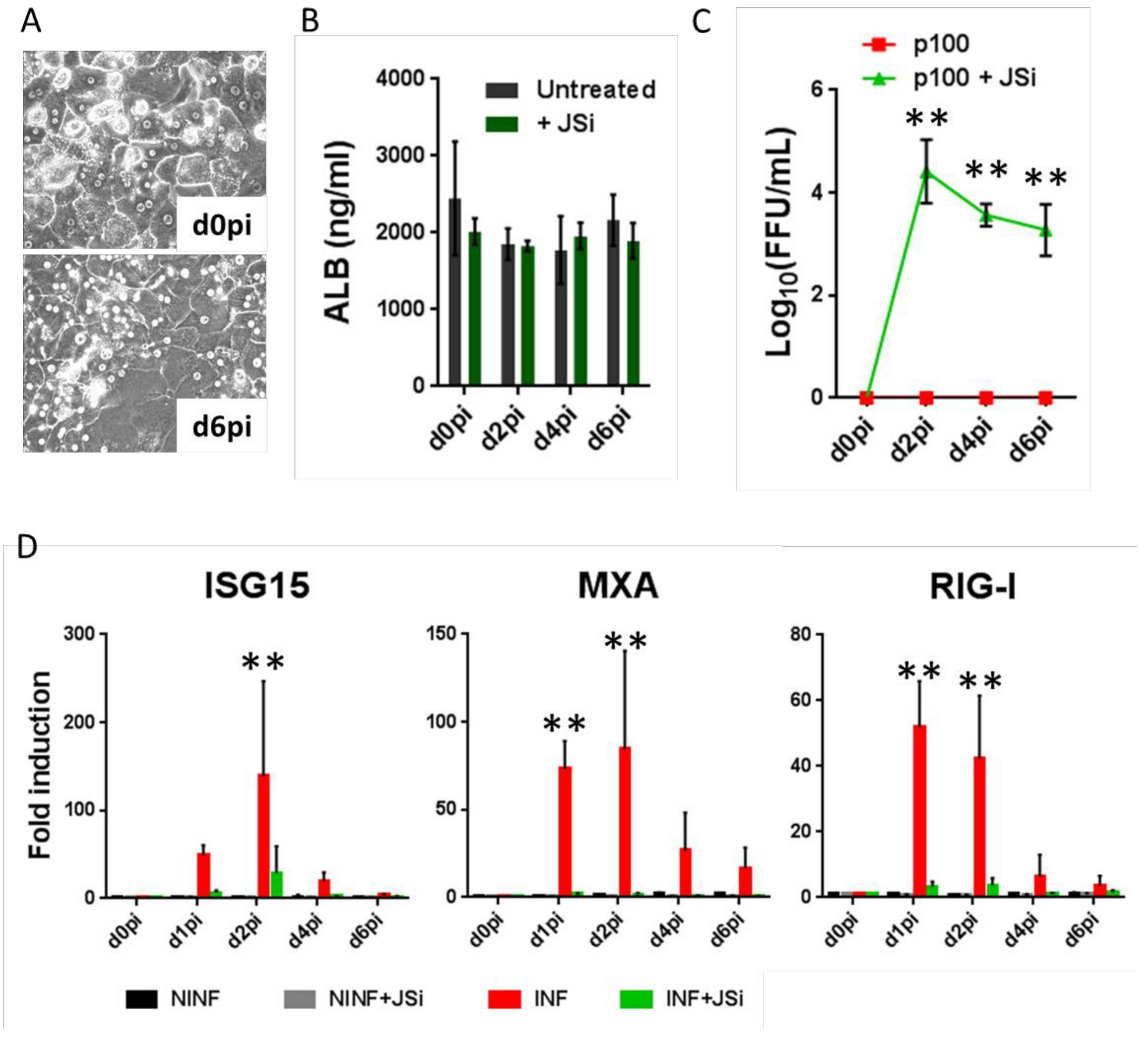

Figure S9: Pathway analyses were performed on the top 1000 most upregulated genes compared to non infected cells, using STRING and the Gene Ontology (GO) Enrichment Analysis tool. (A) Upon HCV infection of HLCs, the STRING network displays one prominent cluster, highlighted in cyan, containing IRGs and representing the induction of the innate immune response and IFN pathway. In presence of the JAK/STAT Inhibitor Ruxolitinib (B, JSi), or the direct antiviral agent Telaprevir (C, DAA), this cluster is disrupted. A similar cluster of innate immune actors can be visualized in infected PHHs (D), but not in infected Huh-7.5 (E). (F) List of enriched Gene Ontology (GO) pathways in infected HLCs, PHHs and Huh-7.5, calculated using the GO Enrichment Analysis tool. Histograms illustrate p-value calculated with Bonferroni correction. Dotted line indicates p-value of 0.05. More info concerning the GO pathway analyses can be found in Table S2.

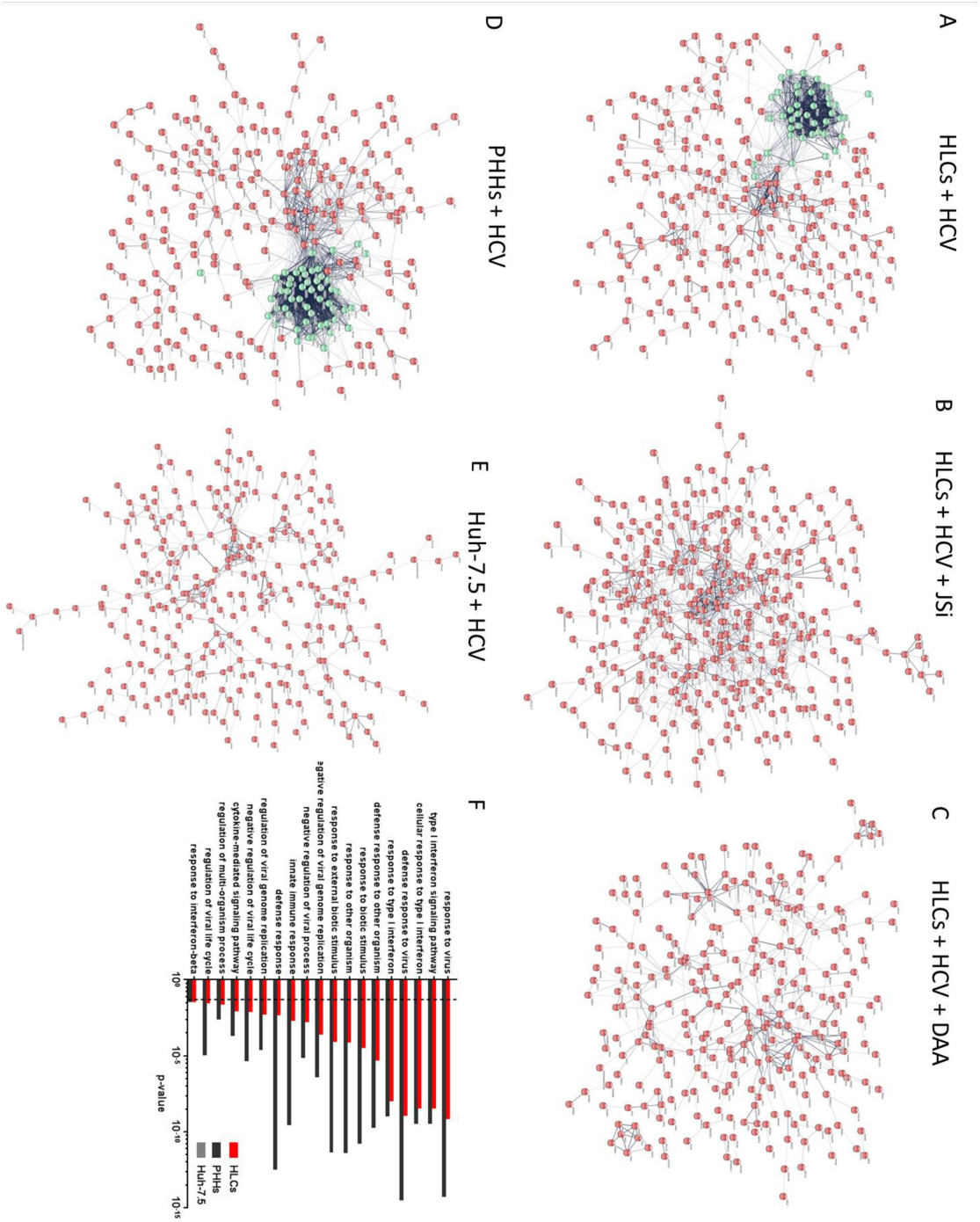
A
HLCs + HCV
B
HLCs + HCV + JSi
C
HLCs + HCV + DAA
D
PHHs + HCV
E
Huh-7.5 + HCV
F
response to virus
type I interferon signaling pathway
cellular response to type I interferon
defense response to virus
response to type I interferon
defense response to other organism
response to biotic stimulus
response to other organism
response to external biotic stimulus
negative regulation of viral genome replication
negative regulation of viral process
innate immune response
defense response
regulation of viral genome replication
negative regulation of viral life cycle
cytokine-mediated signaling pathway
regulation of multi-organism process
regulation of viral life cycle
response to interferon-beta
p-value
HLCs
PHHs
Huh-7.5

Figure S10: RNA-seq analysis of HLC innate immune responses. (A) Fold change of expression of 417 analyzed IRGs in p100 infected HLCs (HCV), with or without treatment with 10µM JAK/STAT inhibitor Ruxolitinib (JSI) or Telaprevir (DAA), relative to uninfected HLCs (NINF). Results are expressed as log_{10} fold change in RPKM compared to uninfected HLCs. (B) Fold induction of selected IRGs upon HLCs infection in absence (red) or presence of Ruxolitinib (green), illustrating STA1- independent IRGs. Detailed RPKM values can be found in Table S4.

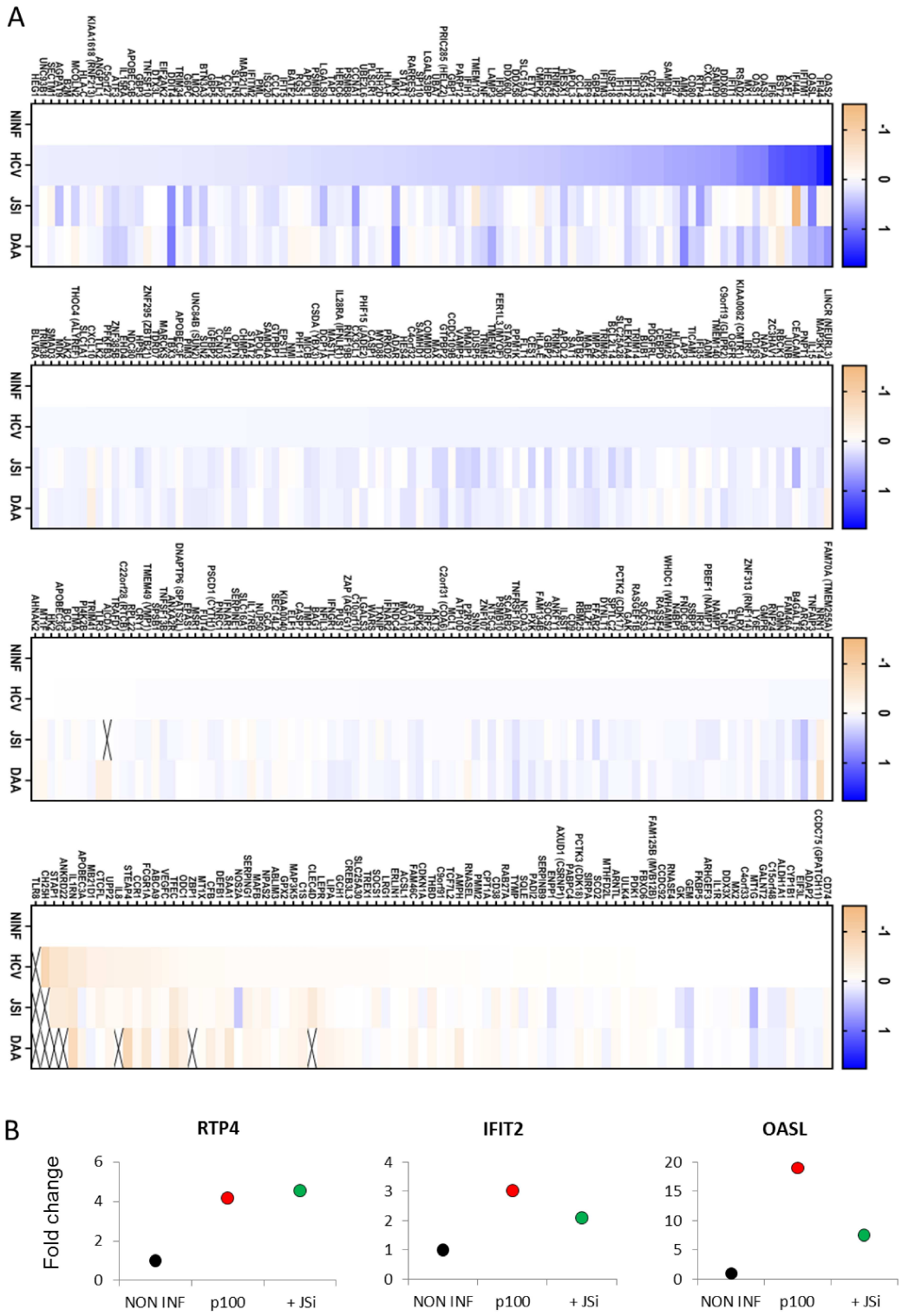
A
NINF
HCV
JSI
DAA
-1
0
1
B
RTP4
IFIT2
OASL
Fold change
NON INF
p100
+ JSi

Figure S11: Long term culture of HLCs. (A) Expression of hepatic markers, assessed by qRT-PCR, (B) albumin (ALB) secretion, assessed by ELISA, (C) CYP3A4 metabolic activity, and (D) secretion of the apolipoproteins (Apo) B100 and E, assessed by ELISA, in 3 weeks long culture of non-infected HLCs, in presence or absence of Ruxolitinib (JSi).

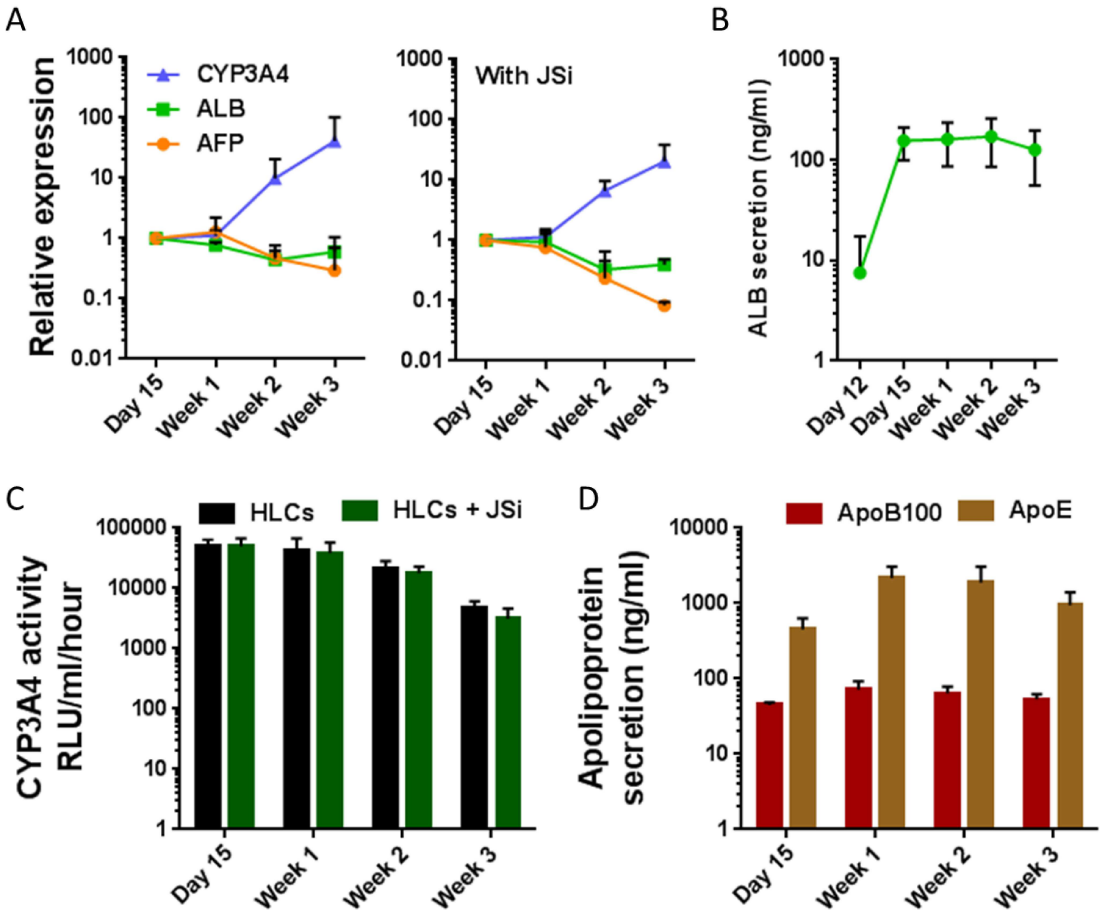

Figure S12: Type III IFN genotype sequencing on genomic DNA isolated from H9ESC. Specific portion of the type III IFN gene were amplified by PCR and sent for Sanger sequencing, revealing genotypes for the SNPs rs12979860(C/T), rs368234815(TT,ΔG), rs8099917(T/G) and rs117648444(C/T). H9ESC are homologous for the non-favorable rs12979860(C/T) T allele, [s11] and heterologous for the rs8099917(T/G) SNP, with the T protective allele believed to improve IFNL3 stability. Interestingly, their rs368234815(TT/ΔG) SNP is homologous for the non-favorable ΔG allele,[s12] which leads to the expression of IFNL4, one of these alleles also carrying a P70S substitution (rs117648444(C/T)) [s13] associated with IFNL4 exhibiting altered antiviral activity.

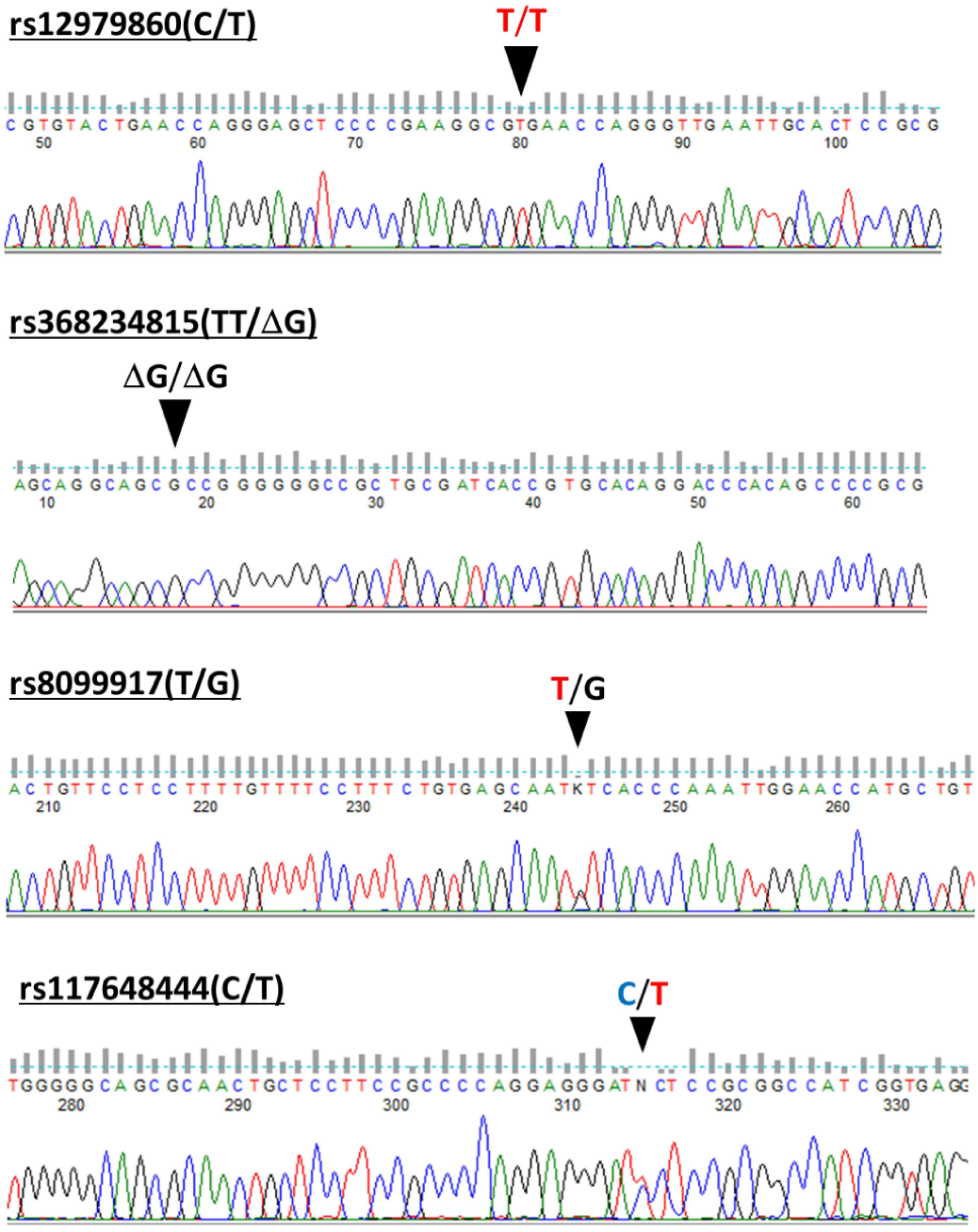
rs12979860(C/T)
T/T
rs368234815(TT/ΔG)
ΔG/ΔG
rs8099917(T/G)
T/G
rs117648444(C/T)
C/T

SUPPLEMENTARY REFERENCES:

s1. Chen KG, Mallon BS, Hamilton RS, *et al*. Non-colony type monolayer culture of human embryonic stem cells. Stem Cell Res 2012; 9:237-48.

s2. Carpentier A, Nimgaonkar I, Chu V, *et al.* Hepatic differentiation of human pluripotent stem cells in miniaturized format suitable for high-throughput screen. Stem Cell Res 2016; 16:640-50.

s3. Kleine M, Riemer M, Krech T, *et al.* Explanted diseased livers - a possible source of metabolic competent primary human hepatocytes. PloS one 2014;9:e101386.

s4. Sheldon J, Beach NM, Moreno E, *et al.* Increased replicative fitness can lead to decreased drug sensitivity of hepatitis C virus. J Virol 2014; 88:12098-111.

s5. Lindenbach BD, Evans MJ, Syder AJ, *et al.* Complete replication of hepatitis C virus in cell culture.Science2005; 309:623-6.

s6. Livak KJ & Schmittgen TD. Analysis of relative gene expression data using real-time quantitative PCR and the 2(-Delta Delta C(T)) Method. Methods 2001; 25:402-8.

s7. Uzé G, Di Marco E, Mouchel-Vielh D, *et al.* Domains of interaction between alpha interferon and its receptor components. J. Mol. Biol. 1994; 243:245-7.

s8. Szklarczyk D, Gable AL, Lyon D, *et al.* STRING v11: protein-protein association networks with increased coverage, supporting functional discovery in genome-wide experimental datasets. Nucleic Acids Res 2019; 47:D607-13.

s9. Ashburner M, Ball CA, Blake JA, *et al.* Gene ontology: tool for the unification of biology. Nat Genet 2000;25:25-9.

s10. The Gene Ontology Consortium. The Gene Ontology Resource: 20 years and still GOing strong. Nucleic Acids Res. 2019; 47:D330-D338.

s11. Wu X, Dao Thi VL, Huang Y, *et al*. Intrinsic Immunity Shapes Viral Resistance of Stem Cells. Cell 2018; 172:423-38.

s12. Thomas DL, Thio CL, Martin MP, *et al.* Genetic variation in IL28B and spontaneous clearance of hepatitis C virus. Nature 2009; 461:798-801.

s13. Prokunina-Olsson L, Muchmore B, Tang W, *et al.* A variant upstream of IFNL3 (IL28B) creating a new interferon gene IFNL4 is associated with impaired clearance of hepatitis C virus. Nat Genet 2013; 45:164-71.

s14. Terczyńska-Dyla E, Bibert S, Duong FH, *et al*. Reduced IFNλ4 activity is associated with improved HCV clearance and reduced expression of interferon-stimulated genes. Nat Commun 2014; 5:5699.